

Project Number: ME-RLN-0804

# Redesign of the Cam Dynamics Test Machine

A Major Qualifying Project Report  
Submitted to the Faculty of the Mechanical Engineering Department  
of Worcester Polytechnic Institute  
in partial fulfillment of the requirements for the  
Degree of Bachelor of Science

by:

---

Daniel Morehouse

---

Jon Tashman

May 5, 2009

Approved:

---

Professor Robert L. Norton, Advisor

## Acknowledgements

Special thanks are owed to the following individuals for their guidance and contributions to this project:

Professor Robert Norton

Professor John Sullivan

Neil Whitehouse

Carl Johnson

David Embree

and

Matt Rhodes

We would also like to thank Dynamic Fabricated Products for their generous allowance of our use of their machine shop and time.

## Abstract

The Cam Dynamics Test Machine (CDTM) was made to demonstrate cam operation and to test the dynamics of industrial cam-follower systems. Recent modifications to the CDTM made it inoperable in a classroom setting and revealed damage-causing flaws in the initial design. This project encompassed the redesign of the follower train assemblies in the machine to eliminate interference between the follower arms and the cams. This was accomplished by straddle-mounting the follower roller within a well in the new follower arm. The newly designed follower train and accompanying parts were analyzed using dynamic modeling and finite element analysis, and the follower arm width was optimized for minimal deflection at the maximum rotational speed of the cam shaft. This project also added the capability of powering the machine in a classroom, improved the safety and fidelity of the electrical wiring configuration, and added storage space. Finally, the sensing equipment was connected to a data acquisition board, and a Virtual Instrument was written to interpret the output signals of each of the machine's sensors to aid future experimentation.

# Table of Contents

1. Introduction.....	1
2. Background.....	3
2.1 Converting between Rotational and Other Forms of Motion .....	3
2.2 The Cam Dynamics Test Machine.....	5
2.2.1 The Cams .....	11
2.2.2 The Motor and the Frequency Inverter .....	12
2.2.3 Instrumentation .....	15
2.2.3.1 The Torque Transducer.....	15
2.2.3.2 The Accelerometers .....	16
2.2.3.3 The Optical Encoders.....	16
2.2.3.4 The Linear Velocity Transducers.....	17
2.2.3.5 The Linearly Variable Differential Transformers .....	18
2.2.3.6 The Power Supplies .....	19
2.3 Theory.....	19
2.3.1 Electrical Interference .....	19
2.3.2 Finite Element Analysis.....	20
2.4 Software .....	21
2.4.1 ProEngineer.....	21
2.4.2 ANSYS .....	21
2.4.3 ANSYS Workbench.....	21
2.4.4 DYNACAM.....	21
2.4.5 LabVIEW .....	22
2.5 Restrictions of Digitally Acquiring Data .....	22
3. Design .....	25
3.1 Specific Requirements .....	25
3.1.1 Product Specifications .....	25
3.1.2 Design Goals .....	26
3.2 Redesigning the Follower Train.....	26
3.2.1 Bearing Selection .....	27
3.2.2 The New Follower Arms .....	29
3.2.2.1 Iterative Finite Element Analysis Procedure .....	30
3.2.2.2 Weight Reduction .....	31
3.2.2.3 Design of the Other Follower Train Elements.....	32
3.2.2.4 Width Optimization .....	37
3.3 Improving Experimentation and Classroom-Readiness.....	39
3.3.1 Creating the Virtual Instrument .....	41
3.3.2 Operability in Classrooms.....	43
3.4 Improving the Electrical and Storage Configurations .....	44

3.4.1 The New Mounting and Storage Plan .....	44
3.4.2 The New Wiring Configuration Plan .....	52
3.4.3 The New Motor Control and Input-Output Panel .....	57
4. Realization and Results .....	60
4.1 Wiring of the Sensors.....	66
5. Conclusion .....	68
6. Recommendations.....	68
7. References.....	70
Appendix A: Validation of the Finite Element Analysis .....	72
A.1 Validation of the Software Value.....	72
Appendix B: Axial Spacing in the New Design .....	77
B.1 Roller Bearing within the Follower Arm Well.....	77
B.2 Con-Rod - Follower Arm Connector within the Follower Arm Well.....	78
B.3 Follower Arm within the Pivot Block Well .....	79
Appendix C: Purchased Parts.....	80

# 1. Introduction

Students can learn a great deal from academic theory, but their understanding and training is incomplete without experience in realization and practical experimentation. Many of the projects carried out at Worcester Polytechnic Institute by the students and faculty embody a dedication to both theory and practice, and they do so through both their methods of completion and through the intended use of the products of their labor. One such project was the design and construction of the Cam Dynamics Test Machine (CDTM), which was made to demonstrate what cams are and how they function in industry, and was also intended to serve as a platform for cam experimentation and data gathering.

Several changes have been made to the machine since it was first built, most notably the exchange of the old motor for a new, more powerful one. Due to the changes that were made, the machine is now capable of maintaining higher torques and shaft speeds. It was these changes however, along with some initial design flaws, which left the machine in a state of disorder. At the outset of this project, the cantilever design of the follower arms had led to serious wear on the arms and cams because of the unwanted contact between them during use. The wires underneath were scattered and open, and there was no protective housing for the power supply to the sensors. The new motor required 220V, three phase AC power and between 12 and 17 amps of current, more power than could be provided by typical 120V wall power outlets, removing the usefulness of the device as a teaching tool in most classrooms. The control panel for the new motor was very large and could not be mounted on the front panel in place of the old one, so it was placed haphazardly on a plastic sheet in the base of the machine along with its long power cable and connector.

The issues caused by the modifications during recent project work exacerbated the flaws that were present in the initial design, such as the lack of mounting for electronic parts or storage space, as well as the cantilever design of the cam follower trains, revealing room for improvement of the CDTM. The goal of this project was to address those shortcomings

by a redesign of its major components in order to make the machine more functional, more useful, and safer electronically.

Three main objectives for this major qualifying project were developed based on this goal of redesign:

- 1.** Design a new follower train to significantly reduce moments on the follower arm and to prevent contact between the moving elements and the base plate.
- 2.** Modify the power inputs to make the device operable in the classroom and make its data readouts more readily accessible for demonstration and experimentation.
- 3.** Make the electronic configuration safer and better organized and add storage compartments so that tools and accessories to the device can be kept onboard.

## 2. Background

This section of the report details the specific information relevant to this project, including information regarding the CDTM's physical structure, its electrical configuration, and the broader topics touched on by this work.

### *2.1 Converting between Rotational and Other Forms of Motion*

In many industrial situations, it is useful to transform pure rotational motion into a more useful or specific type of motion. Electric motors which are commonly used to actuate an industrial assembly or assembly line can rotate at varied speeds, but that is the limit of their ability. To convert the rotation of the shaft output of a motor, linkages and cams are most commonly used. A linkage is a system of rigid links joined at joints, and can have four or more links and many different types of joints. An example of linkage use is the scissor-lift, where a shaft turned by a motor at the base causes a platform to rise due to the changing angles of the links connected to it, as shown in Figure 1:



Figure 1

Sometimes, an approach that uses cams is more useful or practical than a complicated linkage for transforming rotational motion to translational or oscillatory motion. A cam is essentially a non-circular disc whose surface geometry is dictated by its function. Cams are



also useful in mechanical timing, and they can be used to gain significant mechanical advantage (Munyon). Figure 2 shows some examples of cam geometries.

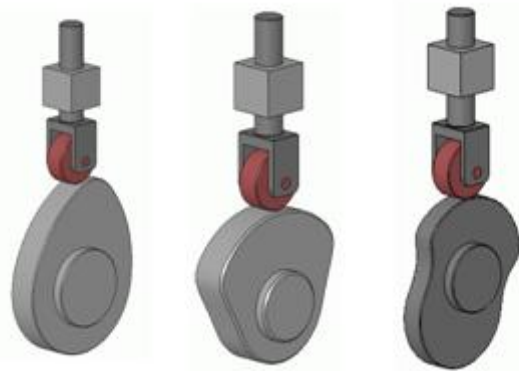


Figure 2 (WikiMedia)

The cams shown are disc cams, and the follower trains shown are direct translating followers. The wheels of the followers are called rollers, and they are held against the cam surface by a spring and forced to follow the changing surface of the cam. The cams are designed in such a way so that they cause the follower train to “rise” (move away from the center of the cam), “fall” (move towards the center of the cam), or dwell (dwells are circular in curvature and they prevent any translation of the follower train). As is illustrated, complex translations can be achieved from a constant rotation of a cam.

Follower trains are often more complex than the translating followers shown above. In some cases, the follower train is a linkage that uses oscillation dictated by the geometry of the cam to perform a useful task elsewhere in a machine. Figure 3 illustrates the distinction between oscillating and translating follower trains (in a simple case):

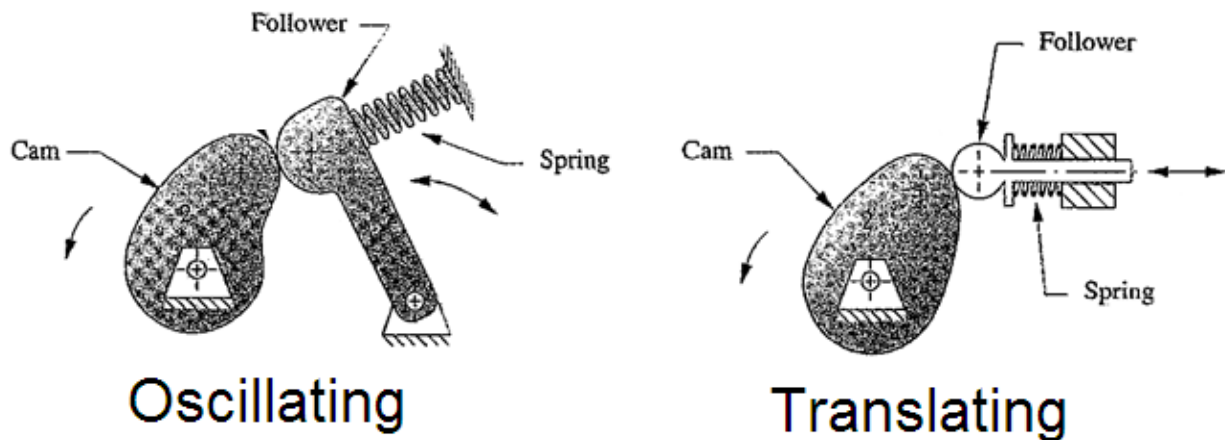
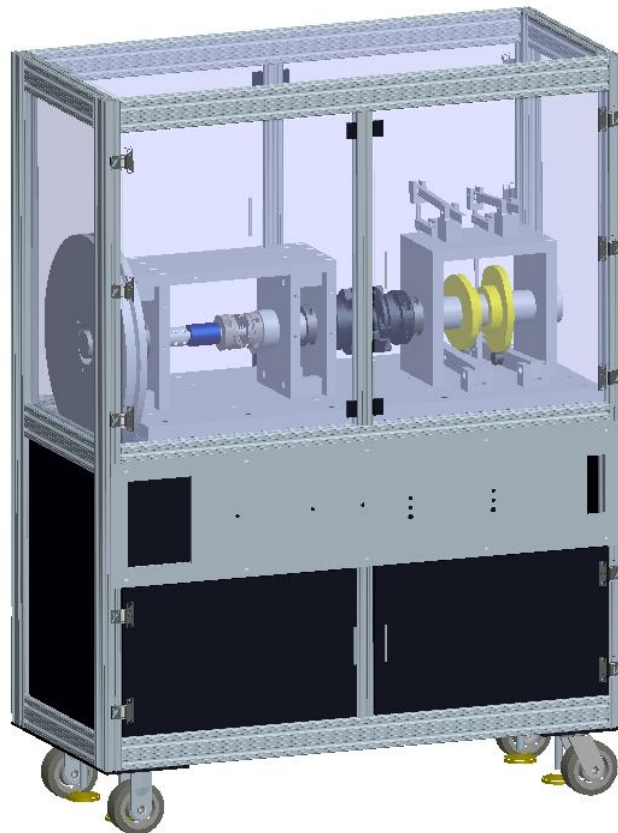


Figure 3 (Norton)

A cam can be as simple as an offset (eccentric) circle, but well-designed cams consider the effect of the surface geometry on accelerations and the rates of accelerations to minimize the potential for non-smooth motion and follower jump (where the roller loses contact with the cam).

## *2.2 The Cam Dynamics Test Machine*

The CDTM was first designed and built by Mathew Munyon, and completed in December of 2006. It was designed to be capable of turning its main shaft at variable speeds to drive two cam-follower assemblies, with one cam designated as the primary cam and the other designed to be a torque-compensating cam. A CAD representation of the machine in its state at the start of the project is shown in Figure 4 below.



**Figure 4**

The upper half of the CDTM is where the moving parts function, and those parts were mounted to one large rectangular base plate at the mid-level. The front of the machine had a panel with BNC outputs connected to the data output lines of each of the nine sensors. The

lower part of the machine, behind its opaque doors, housed the motor and the motor controller along with many of the myriad wires and power supplies needed to run the machine. Figure 5 details the many elements connected to the main shaft that runs the full length of the upper assembly.

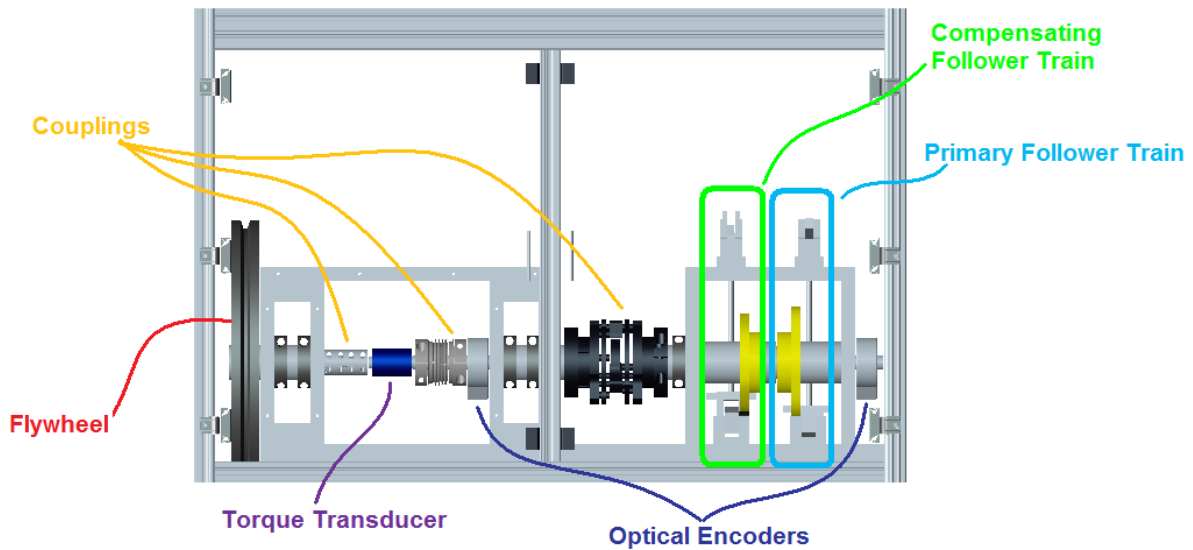


Figure 5

The flywheel weighs about 170 lb, and it is connected by belt to a pulley attached to the motor (which is mounted in the lower half of the frame). The speed of the shaft is reduced by the belt by a factor of five, increasing the torque on the shaft by the same factor. The resulting maximum speed at which the shaft can rotate, irrespective of the maximum speeds that the follower trains can support, is 285 rotations per minute (RPM). The flywheel is shown in Figure 6 below.

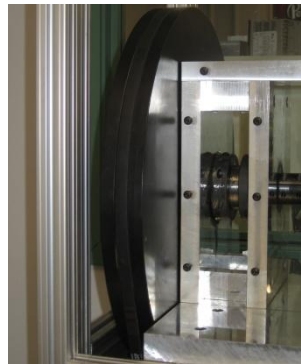


Figure 6

The three shaft couplings ensure transmission of power along the three shaft sections and the torque transducer, and the thrust bearings in the frame pieces along the main assembly keep the shafts horizontal and in line.

Though the profiles of the two cams are different, the follower trains attached to them were identical and oscillating. Figure 7 shows the configuration of the follower trains.

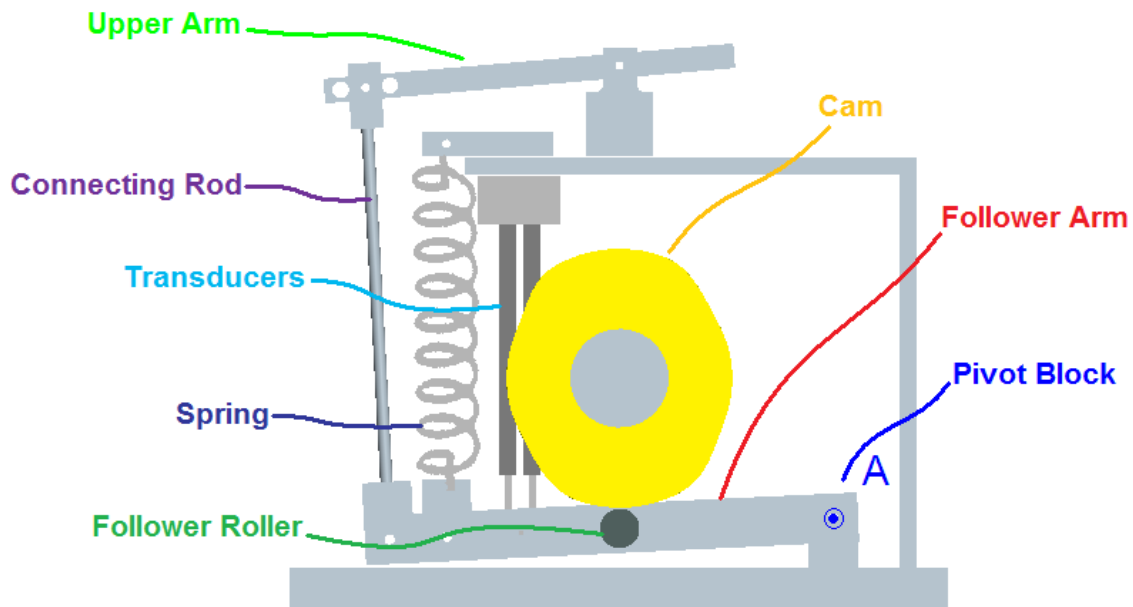


Figure 7

This train was designed so that the follower arm would pivot about a shaft at point A in the pivot block as the cam rotated and forced the follower roller to move up and down along its exterior profile. The follower roller was held against the cam by a spring, pre-tensioned by the two screws shown in orange in the assembly in Figure 8 (which straddled the follower arm).

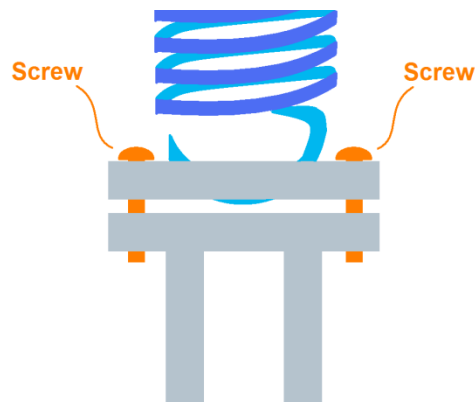


Figure 8

The connecting rod was used to transmit the motion of the follower arm to the upper arm, which in a real industrial assembly would be the output or “business” end. The transducers were connected to the follower arms by a small screw to measure position and velocity.

Though the maximum shaft speed and torque were increased by the addition of the current motor, the follower train was unable to support the higher cam forces present at those higher speeds for two main reasons. First of all, as shown in Figure 9, the follower rollers were cantilevered from the follower arms.

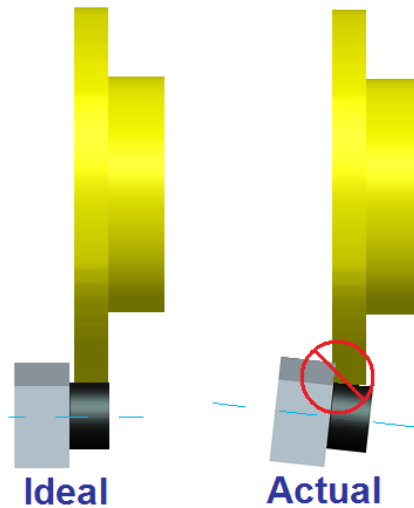


Figure 9

The forces between the roller and the cam were offset from the central plane of the arm, causing a torsional moment that in extreme cases forced the cam to contact and cut away the follower arm. The damage to the cam profile was minimal, but the damage to the follower arm was considerable; that damage is illustrated in Figure 10:



Figure 10

A second flaw in the use of the more powerful motor was that, while a new spring was chosen to hold the follower train against the cam surface, it was not capable of preventing jump at high speeds. The result was that the follower arm would crash into the base plate when the roller jumped off the cam.

The main frame of the machine was composed of extruded aluminum bars from 80/20 Inc, as shown in Figure 11.

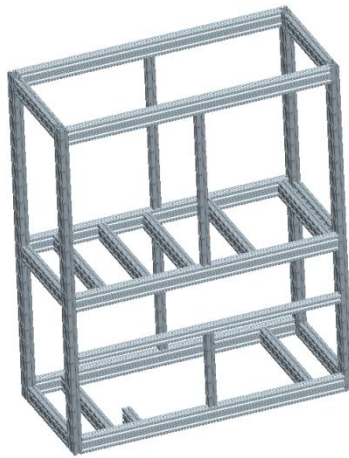


Figure 11

There were casters and retractable stabilizers for mobility and stability, respectively, attached at the base of the frame. The lower half of the machine was enclosed by opaque lexan panels and doors, and housed the motor, motor controller, wiring, belt, and the power supplies.

The wires for power and for sensing were haphazardly attached, many joined chiefly by electrical tape, and one of the power supplies had recently been replaced; it required replacement because the supplies were neither mounted nor enclosed, and someone had dropped a wrench across the terminals while modifying the machine, shorting the circuit. The other power supply was left connected and unenclosed, as shown in Figure 12.



Figure 12

No schematics existed for the wiring, nor was there an explanation of the model numbers and voltage requirements of the sensors or the motor. Figure 13 shows the mounting of the motor and the contents of the lower half of the machine:

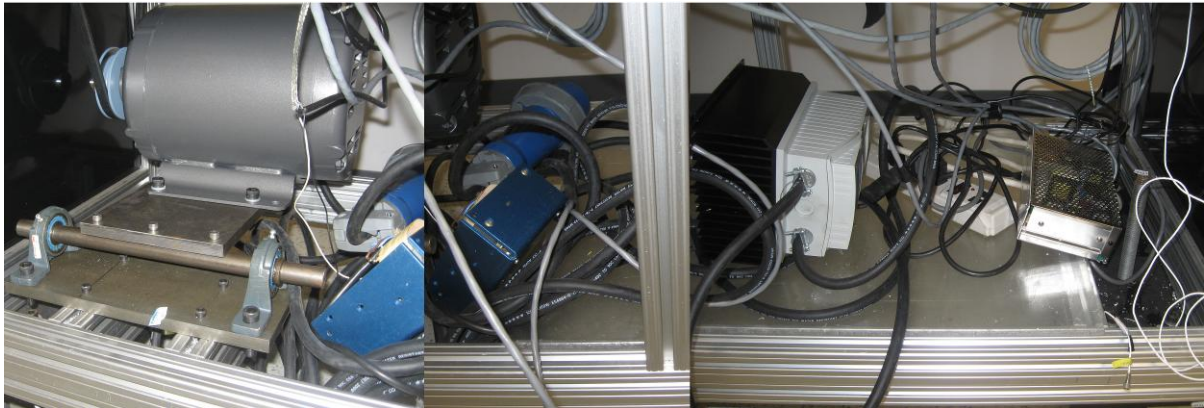


Figure 13

Between the lower half and the functional upper half was the front panel, a large and thin rectangular metal plate with BNC outputs for each of the data lines from the sensors. The motor controller for the newly added motor was much larger than the previous one because of the heat sink on its backside, and could not be mounted in place of the old one on the front panel. As a result, the old controller was left in place in the panel, and its wires remained inside the CDTM. All of the parts in the machine, as well as a full assembly, accompany this report digitally as CAD files. “everything\_with\_drawers1.asm” is the frame and most of the shaft, and “dm\_jt\_asm\_015.asm” is the cam-follower assembly. See Appendix C for a list of purchased parts and their manufacturers.



### 2.2.1 The Cams

Figure 14 shows the two Cams used in the CDTM.

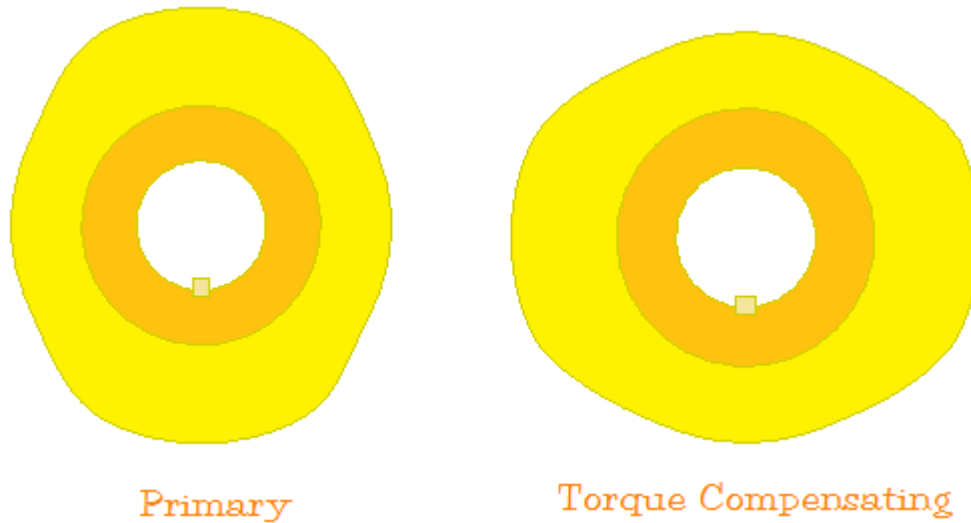


Figure 14

Both are disc cams, and each has eight segments and four dwells. One of them is the primary cam, and is defined as follows:

Initial Cam blank: 7.874in (200mm)

Prime Radius: 4.0625in

Base Circle: 3.4375in

Follower Radius: 0.625in

Table 1: Defining the Primary Cam Profile

Cam Surface Fraction	Rise, Fall, or Dwell	Type of Curve	Starting Radial Distance from Base Circle	Ending Radial Distance from Base Circle
50°	Rise	4-5-6-7 Polynomial	0 in	.5 in
40°	Dwell	Circular Arc	.5 in	.5 in
50°	Fall	3-4-5 Polynomial	.5 in	0 in
40°	Dwell	Circular Arc	0 in	0 in
50°	Rise	Modified Trapezoid	0 in	.5 in
40°	Dwell	Circular Arc	.5 in	.5 in
50°	Fall	Modified Sine	.5 in	0 in
40°	Dwell	Circular Arc	0 in	0 in



The four different curve types used for the rises and falls of this cam are commonly used in cam design, but they are not typically used in creating the same cam profile. They were used in this case because the machine was meant to be used as a teaching tool, and the output data would illustrate the different qualities of the various curve types.

The second is a “Torque Compensating” cam, designed to create opposing torque loading on the camshaft that drives the two simultaneously during operation, significantly decreasing the torque needed to run the CDTM. The profile for the torque compensating cam was generated based on the original cam using DynaCam, a design software explained in more detail in the Software portion of this background chapter.

### 2.2.2 The Motor and the Frequency Inverter

The CDTM camshaft is driven by an AC electric motor. The recently installed motor is a Baldor Industrial M3211-T50 3HP three-phase motor, shown in Figure 15.



Figure 15

Three-phase electricity is used to power the motor because it is the most efficient way to deliver power to an electric motor. Three-phase power is split into three synchronized sine waves separated by 120 degrees in phase. This is so that at any point, the motor will receive power that is close (if not equal) to its peak power (Howstuffworks) – see Figure 16 for an illustration of the three phases of AC power.

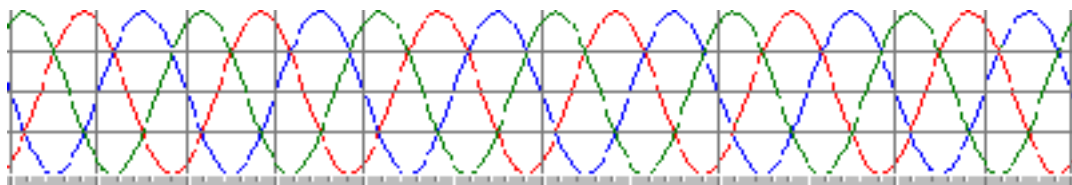


Figure 16

The maximum speed of an AC motor is dependent on the input frequency, voltage per pole, and number of poles.

$$RPM = \frac{V \times f}{p}$$

The result from this equation yields an ideal RPM speed. Comparing this number to what the full load motor RPM is, gives a slip rating. The slip rating is the shaft speed compared to the electro-magnetic lag. For torque generation, this lag is necessary. This motor is capable of 1425 RPM and requires 50Hz power at an input voltage of three-phase 220V.

An important aspect of using the Baldor motor, along with many other AC motors, is the inability to control its speed without an outside control unit. The frequency inverter equipped in the CDTM is a Lenze AC Tech ESV222N02YXC, which is used as a motor speed controller (see Figure 17).



Figure 17

This frequency drive accepts single or three phase utility power at 60Hz. This inverter changes the frequency of the power, thereby altering the RPM output of the electric motor. A benefit of using a frequency inverter is that it controls the amount of current being pulled when starting up the three-phase electric motor. AC electric motors are known to take more than full speed current draw at startup, which can impose a problem on overloading the building's breakers or fuses. With a frequency inverter, when starting up the motor, the frequency is very low, and then slowly increases to full power.

In order to provide three-phase power to the motor, a cable with a heavy-duty four-pin connector was attached to the motor controller. The connector, shown in Figure dsd, was used so that the CDTM could be plugged into the three-phase power ports in the Experimentation Lab which put out enough current (10.8A) for the machine.

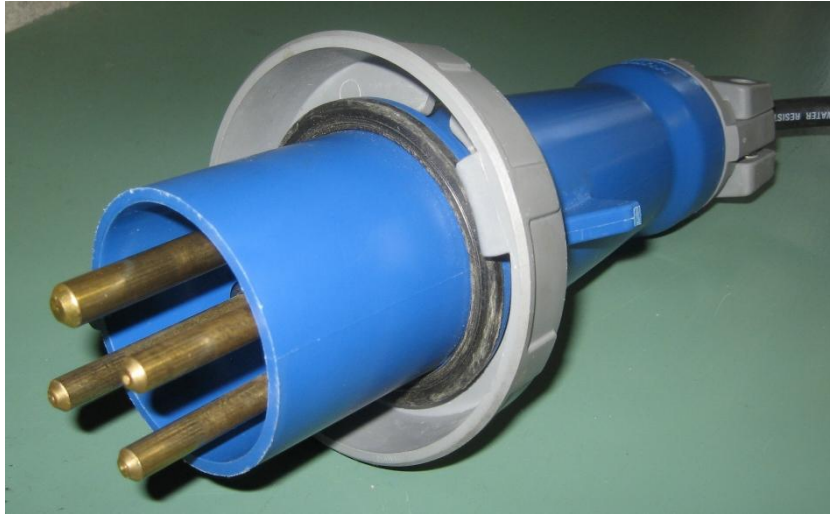


Figure 18

The issue with this type of connector as well as three-phase power is that they are not widely available in typical classrooms, which effectively limited the operation of the CDTM to the experimentation lab.

### 2.2.3 Instrumentation

The Cam Dynamics Test Machine relies on integrated sensors to record various characteristics while testing a cam. These sensors include Torque Transducers, Accelerometers, Optical Encoders, Linear Velocity Transducers, and Linearly Variable Differential Transformers. The various instruments in the CDTM output position, velocity, and acceleration for both the primary and secondary follower trains. There is also shaft data that can be recorded such as the driveshaft position, camshaft position, and torque.

There were ten BNC female connectors mounted on the front panel of the CDTM to allow users access to the data put out by each of the sensors. The front panel is shown below in Figure 19:

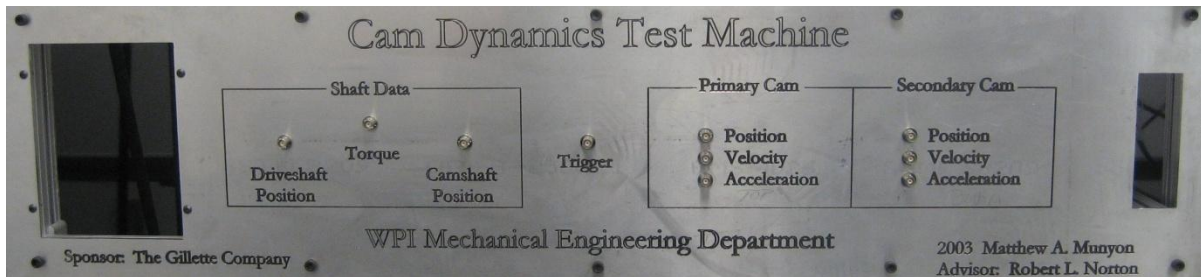


Figure 19

#### 2.2.3.1 The Torque Transducer

The torque transducer mounted in-line with the shafts on the CDTM is an LXT 971 from Cooper Instruments, and is shown in Figure 20:

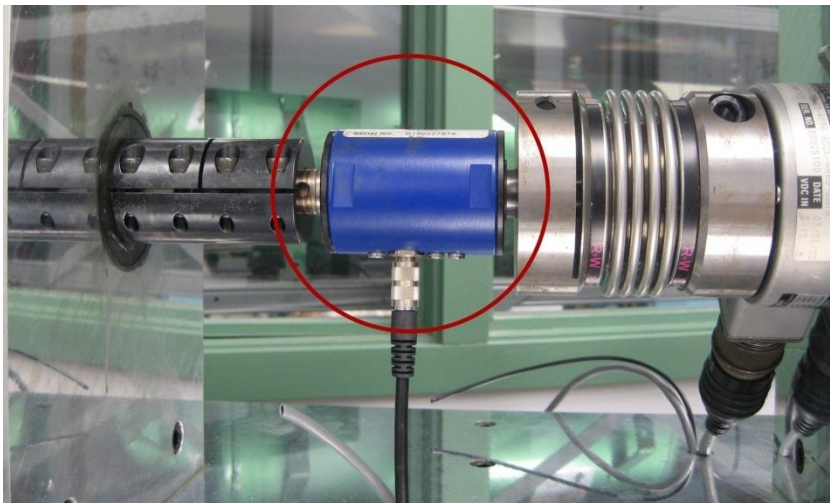


Figure 20

Non-contact sensors within the transducer detect the magnetic field as it changes due to the torque applied to the shaft, and the sensors output voltage signals that vary with the torque (Cooper Instruments).

This transducer requires between 9V and 12V DC power to operate, and outputs voltage signals between 0.5 and 4.5 V DC corresponding to the torque.

### **2.2.3.2 The Accelerometers**

Accelerometers are sensors that measure the accelerations on an object. Accelerometers can be made to measure 1, 2, or 3 axes. They also come in two different types, one being high pass and the other low pass. High pass accelerometers output directly to the measurement instruments, making them very accurate. High pass accelerometers are useful for high temperature environments where low pass accelerometers would not be able to function (in excess of 150 degrees Celsius due to electrical circuit temperature limit in low pass accelerometers). Low pass accelerometers are made with a charge exciting accelerometer and use an FET (field-effect transistor) to convert the charge to a more usable voltage. This method is easier to interface with more mainstream testing equipment (OMEGA). Low pass accelerometers are more common but are not able to clearly read high frequencies. This makes them useful for low acceleration applications. The common sensitivity ratings for low pass accelerometers are 10 mV/g and 500 mV/g, where sensitivity is higher as the number goes up. It is also important to note when these sensors are to be mounted on a spongier surface can act as a dampener and reduce the sensitivity of the accelerometer (OMEGA).

The Dytran 3145A accelerometers used in the CDTM do not require voltage inputs, but they do require a current source; they were connected to the Dytran 4114 Current Source, which put out BNC to data cables that then ran to the front panel. These particular accelerometers output 100 mV/g (g refers to gravitational acceleration).

### **2.2.3.3 The Optical Encoders**

Optical Encoders are necessary for finding the position of the shaft near both the flywheel and the cams to measure the torsional deflection along the shaft. Optical encoders work by shining a light through a disk with gaps (also known as tracks) to let the light

through while having a photo sensor on the other end that reads these patterns at a very fast rate (see Figure 21).

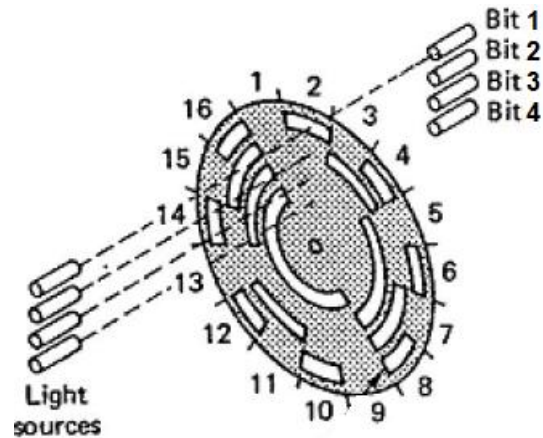


Figure 21

When two encoders are used in conjunction, a timing system can be setup to measure the relative change in position (Northeastern). An encoder is rated in lines per revolution. The greater the lines per revolution, the more accurate the device is.

The encoders of the CDTM are from BEI Technologies, are incremental (relative to start position) encoders, and are shown in Figure 22 below:



Figure 22

These encoders require between 5V and 15V DC, and their output signal alternates between the input voltage and zero in square wave form. These encoders produce 4096 square waves per rotation of the shaft, as well as a once-per-revolution “trigger” pulse.

#### 2.2.3.4 The Linear Velocity Transducers

Linear Velocity Transducers (Figure 23) work by acting as a simple generator. These sensors do not require any input voltage; instead they create a voltage that is linearly

proportional to the speed of the moving part they are attached to. A magnetic rod (shown on the left of the figure) on the inside of the LVT is surrounded by a coil of wire, and it creates this current naturally as it moves up and down.



Figure 23

The two LVTs that move along with the follower trains on the CDTM are made by TransTech (Model 0112 0000), and they produce 550 mV/in/sec.

### 2.2.3.5 The Linearly Variable Differential Transformers

Linearly Variable Differential Transformers (LVDTs) are similar to Linear Velocity Transducers in that they involve a rod moving up and down inside a hollow shaft. They measure position rather than velocity, and they do require a voltage input in order to function. LVDTs work by splitting up a hollow cylinder into three sections of electrical coil. The voltage input powers the center coil as the rod moves up and down, and responds to the changing ratio of contact between all three coils and the rod. Figure 13 shows a cut-away view of an LVDT, as well as a picture of the LVDTs in use in the CDTM.

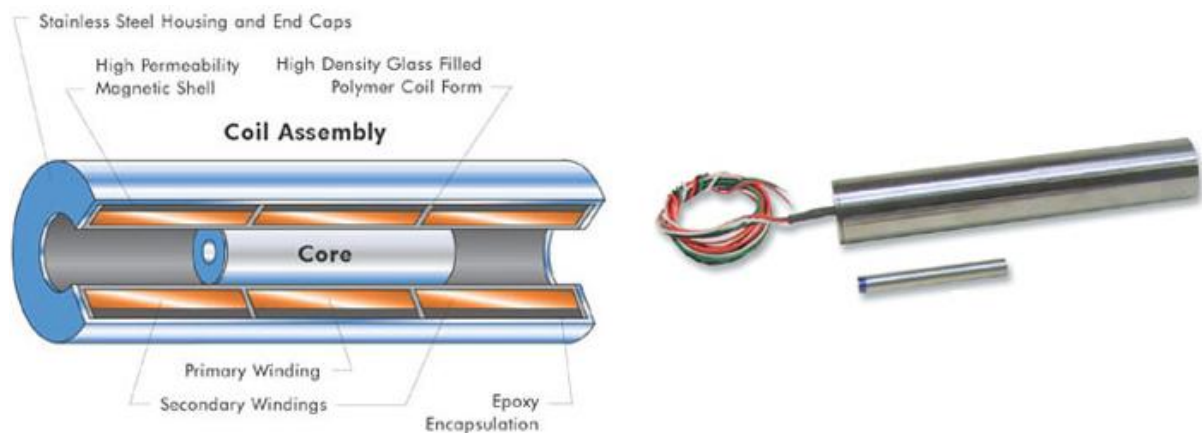


Figure 24

These LVDTs, made by Macro Sensors, require  $\pm 15V$  DC power, and put out 20V/in.



### 2.2.3.6 The Power Supplies

Power supplies were included in the original design in order to convert wall AC power into the various voltage needs of the sensors, as described previously. The two power supplies in the CDTM at the outset of this project are shown in Figure 25:

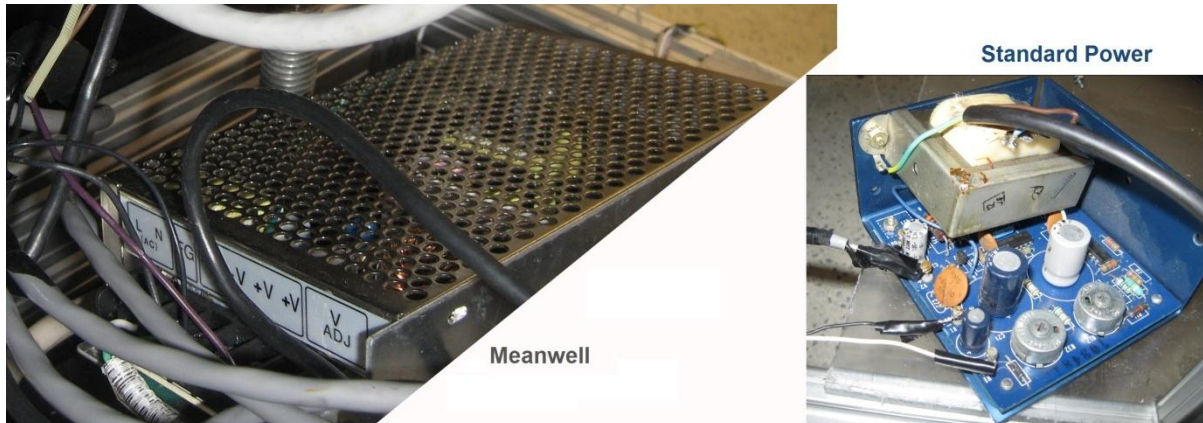


Figure 25

Both accepted and were powered by 120V AC power (typical of any residential wall socket). The blue supply, made by Standard Power, output 13.6V DC and 5V DC. The silver supply, made by Meanwell, output two isolated circuits of 12V DC.

## 2.3 Theory

### 2.3.1 Electrical Interference

Managing output data from sensors requires that attention be put towards avoiding electrical interference and losing signal because of excessive cable length. While signal degradation is minimal over short distances (less than three feet) for carrying analogue signals, proximity to voltage sources can create electrical interference and engender false readings from measuring equipment.

To minimize these occurrences, shielding the data wires and having the shield's conductor grounded will shunt electrical interference into the ground. When dealing with digital signals such as USB, interference and cable length differ. Interference is normally eliminated because of USB's shielded cable. USB cable length is limited to 16 feet. This can be extended by a factor of five by adding five USB hubs, which boost the signal.



### 2.3.2 Finite Element Analysis

In order to analyze and characterize the ability of a part or system that is more complex than a simple extruded shape to maintain form and function under the expected loading and conditions of its use, finite element analysis (FEA) can be performed. The main idea of FEA is to break down the part or system into smaller, simpler parts (“elements”) with easily defined characteristics such as elasticity or thermal conductivity, depending on the analysis. The part or system is then rebuilt using these small parts through a process called meshing, connecting the “elements” at points called “nodes”. Typically, the more elements that a part is broken into, the more accurate the resulting solution can be. FEA can be applied to models in two or three dimensions, and can also be applied to time-dependent problems.

Originally, FEA had limited applications because of the great number of calculations required to complete it with a significant-enough number of elements. With the advent of modern computing, FEA has become not only more feasible but also more reliable and accurate. While computers have solved the problem of carrying out complex and lengthy calculations quickly, any FEA is only as powerful or correct as the creator makes it; the proper set-up of an FEA is critical to its utility.

A typical FEA can be broken into five steps. The first step is discretization, where the types of elements, number of elements, and number of nodes is chosen and the model is meshed into elements. The second step is the construction of the element equations, typically relating the deformation of the elements to their stiffness. The third step is to combine those individual equations into one large system equation matrix; in the case of deformation analysis, the matrix is referred to as the stiffness matrix. The second and third steps are often behind-the-scenes in commercial software. The fourth step, arguably the most critical, is the application of boundary conditions and loading. These can include point loads, distributed loads (pressures), and displacement constraints. The fifth and final step is to evaluate the unknown parameters of the system equation with the loading and boundary conditions applied, and then to find other parameters based on the original parameters. For example, in the case of a stiffness matrix, the unknowns are deformations, and once the deformations are solved, they can be used to find the stress.

## **2.4 Software**

### **2.4.1 ProEngineer**

In order to understand the individual parts of the machine and how they fit together, and then to design and analyze new parts and check how they would fit and function within the machine, CAD models were built of every piece of the CDTM. This was accomplished using ProEngineer Wildfire 4.0. It is the newest version of ProEngineer, a three-dimensional solid modeling software. After the models were built, they were assembled into sub-assemblies as well as a top-level assembly of the entire device, and design drawings for the parts were made. ProEngineer facilitated robust 3D modeling and dimensioning the drawings.

### **2.4.2 ANSYS**

One of the finite element analysis packages used to assess the new parts, ANSYS 11 has both the tools to model parts and systems as well as the ability to import wireframe and solid models. It is capable of generating mesh, and has a thorough database of element types for all manner of engineering analyses. Importing solid models is more complex in ANSYS than building them node-by-node or element-by-element, and it is quick to use for simple analyses.

### **2.4.3 ANSYS Workbench**

ANSYS Workbench is a more CAD and stress-analysis based version of ANSYS that makes the development of three-dimensional constraints and the importing of CAD models more streamlined and user friendly. Workbench includes preset boundary conditions to choose from and apply. Workbench is limited in the number of elements and the amount of control the user has over the meshing, so the original version of ANSYS is better suited to advanced designs, but Workbench was capable of handling the types of analysis performed in this project.

### **2.4.4 DYNACAM**

A tool for designing and outputting cam profiles, as well as for analyzing the dynamics of cam-follower systems, is DYNACAM. It can be used to define each segment of a cam, and to then investigate graphically and mathematically the position, velocity,

acceleration, and jerk functions associated with the profiles generated. It can generate the profile of a torque-compensating cam to match the designed cam, and the user can output either profile in a format readable by CAD and CAM software packages (a set of points describing the profile).

Another distinguishing feature of DYNACAM is the ability to design follower trains and roller dimensions in order to fully characterize a system. Start angles, speeds, and eccentricities can all be defined. DYNACAM determines when and if jump will occur, and can estimate the effect of vibrations on the forces transmitted.

#### **2.4.5 LabVIEW**

LabVIEW is a software package created by National Instruments. It is used in industry to read data from sensors, to write data to spreadsheets, and to display real-time graphical illustrations of the instruments it reads. It is often used as an aid to experimentation. LabVIEW files are called Virtual Instruments, and are composed of both a Front Panel and a Block Diagram. The Block Diagram is a graphical programming tool, allowing the user to select input and output instruments and program their functionality. Some items on the block diagram are used to link to the front panel, the primary display and functional control of a VI during use. The front panel can show graphical displays of the data being collected, and can also have “on/off” switches, text fields, and other types of controls. Instruments that are used in experimentation but not directly connected to the computer that a VI is hosted on are often connected to it via Data Acquisition devices (DAQs), which can have both inputs and outputs. The VIs created and tested in this project were programmed using LabVIEW Version 8.0.

### ***2.5 Restrictions of Digitally Acquiring Data***

Data Acquisition devices (DAQs) provide a useful interface between a computer and the sensors used in experimentation. DAQs are normally characterized by the number of inputs and outputs (I/Os) available, the variety of the I/Os (such as analog and digital), and the sampling rate they are able to maintain.

WPI’s data acquisition technology is mainly National Instruments hardware, and the equipment in Higgins Labs Experimentation Lab was investigated first. The DAQs installed

in the lab consisted of a National Instruments SCXI-1122 paired with a SCXI-1322, and both are shown in Figure 26:

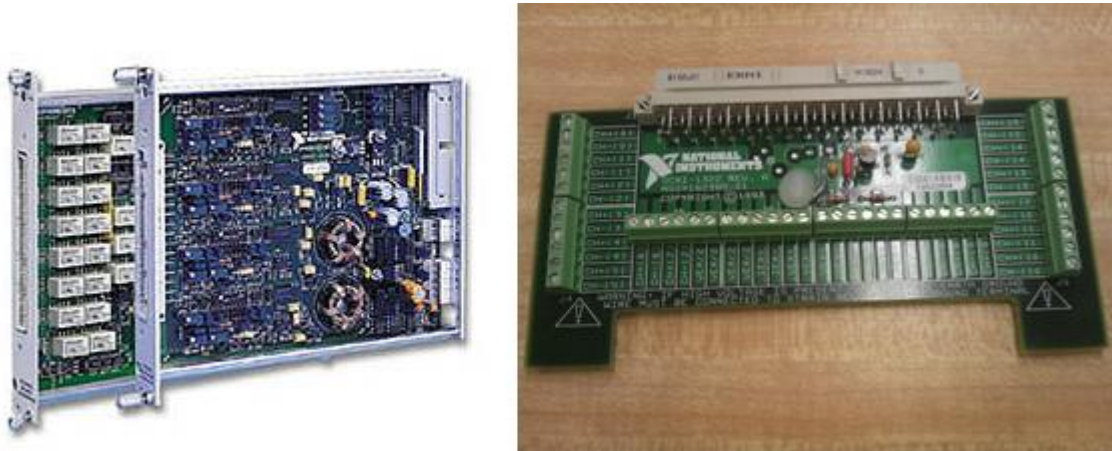


Figure 26

The SCXI-1322 was a termination card that allows sensor outputs to be screwed in, which was then plugged into the SCXI-1122. While the maximum input voltages were well within the desired range ( $-250\text{V}/250\text{V}$ ), the sampling speeds of these devices were low (100 samples per second). Acquiring data at those speeds would be adequate for one sensor at a low RPM of the camshaft, but this rate would be too slow to read ten sensors at camshaft speeds of 260 RPM. Using these DAQs would also have limited data acquisition to taking place in HL031, and the initial set-up of data communication from the CDTM to the SCXI-1322 would be cumbersome due to the need to screw in each lead.

An alternative also present in Higgins Laboratories was the NI BNC-2120, shown in Figure 27:



Figure 27

The BNC-2120 is an adapter block that allows BNC connection to its analog inputs. The sample speed relied on the speed of the interface card that it would connect to a desktop PC. Unfortunately there were three issues with this device. Currently none of the M series PCI DAQ cards were installed in the lab so that the BNC 2120 could operate correctly. The second problem was that there were only eight analog inputs for this adapter block. The third was that the data collection would be limited to desktop PCs.

A further restriction was that portable PCI cards were expensive and atypical for laptops, making it difficult to use the existing equipment in a classroom setting outside the lab with any computer available. Using lab computers would have caused additional issues besides non-mobility; the equipment in the lab is occasionally upgraded and it is likely that future upgrades would not have been compatible with a solution for the CDTM based on the current equipment in the lab. For example, if the communication to the computer was by PCI, but after a few years of upgraded computers, only PCI-E interfaces could be utilized, a new DAQ would have to be purchased that would be accepted by the new communication standard.

The restrictions inherent in using the lab equipment effectively prevented data collection outside of the experimentation lab, limiting the machine's use. The desire to expand the machine's potential for data collection and display motivated a search for a new DAQ that could be dedicated to the CDTM, and that search is described in greater detail in Section 3.3.

## 3. Design

The findings of research into the fundamental concepts of the device's operation, the computer-aided modeling of all of its individual parts, and an investigation of the needs and outputs of its many sensors led to a more fully developed plan for the completion of the three major design objectives. Those objectives were to redesign the follower trains, to improve data collection and classroom use, and to reorganize the electrical and storage configurations of the CDTM.

### 3.1 Specific Requirements

In order to constrain the redesign of the CDTM, guidelines were developed in the form of product specifications and design goals. The product specifications were rigid guidelines based on research and client requirements, and the design goals were aspirations which, if achieved, would expand or improve the machine.

#### 3.1.1 Product Specifications

- The material used to create the new follower arm should be consistent with existing parts (Aluminum 6061-T6)
- The CDTM must contain all of the necessary tools to service it, as well as spare parts
- The power supplies must be enclosed and mounted such that shock to users and damage to the supplies are both prevented
- The original cam shaft and cams must be maintained
- The new follower trains must not allow contact between the follower arms and the cams
- The new follower arms should include a well for the roller such that the arm straddle-mounts the roller
- The primary follower arm must not deflect more than 0.005" at the con-rod end.<sup>†</sup>

<sup>†</sup> Critical stress levels typically engender larger part deflections. Limiting the deformation to a small value is a means of ensuring that the stresses developed in the part are not damaging.

### 3.1.2 Design Goals

- The CDTM must be made capable of operating in a classroom environment
- The motor controls should be made easily accessible and safe for the operator
- Readouts for demo and experimentation purposes should be made visible through the development of a Virtual Instrument capable of running on any pc with LabVIEW
- An improved method of attaching and tensioning the springs in the follower trains should be developed, making changing springs safer and less prone to error.
- Drawers to contain tools, spare parts, and add-ons for CDTM should be built

### 3.2 Redesigning the Follower Train

The aim in redesigning the oscillating follower trains, one of which followed each cam, was to reduce friction and damaging contact between all moving parts. To narrow the number of variables in the design of the new parts, several of the old ones were maintained, such as the upper arms and pivots, the con-rod connector, and the part that connected the upper arm and the con-rod and allowed them to pivot at a pinned joint. The two transducers attached to each train and the sub-assemblies that mounted them were also re-implemented in the new design, along with the brackets that mount the springs to the top of each enclosure. Originally, as shown in Figure 28, the parts connecting the springs and the con rods to the arms were also to be used.

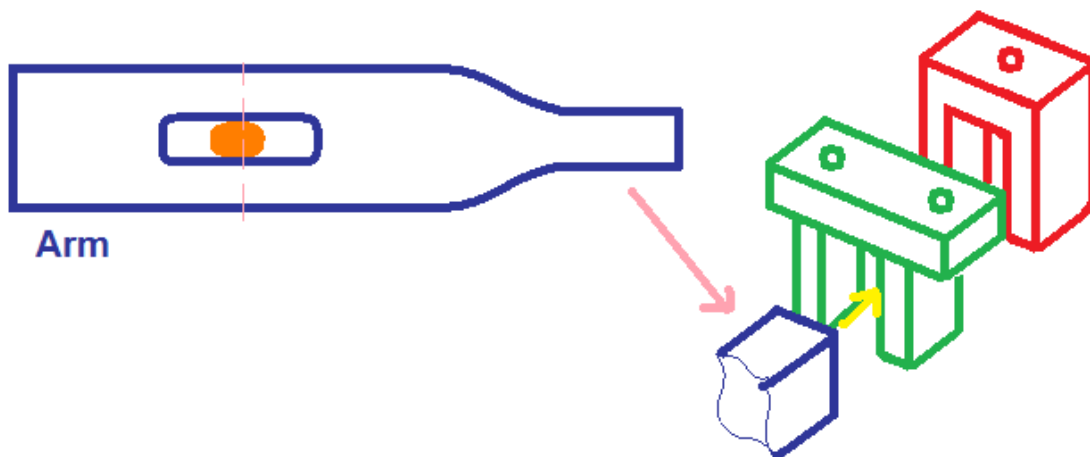


Figure 28

Several factors prohibited the re-use of these connectors to the arms. A significant issue was that the arms needed to be both wide enough to house the roller and narrow enough to accept the connectors, and this was not as manufacturable or as strong as a rectangular prism of constant width. Also, the plan to put the rollers (and thereby the arms) in-line with the cams meant a narrower gap between the arms, making it difficult for these parts to fit side-by-side unless they were modified.

In addition to using existing parts where possible, many dimensions were also preserved where possible in the new part designs. For example, the distance from the pivot to the roller, to the spring attach point, and to the con-rod pivot were all consistent with the old trains. Almost every part of the two trains, including the structural parts, was based in some way on the shape and size of the follower arms, placing the priority of redesign on the arms themselves. The arms were dependent upon the selection of new roller bearings to replace the cantilevered ones used in the old trains.

### **3.2.1 Bearing Selection**

In cam design, a critical concern is the size of the roller radius relative to the curvature of the cam profile. The radius of the roller bearing needs to be small enough to completely follow the cam surface, but large enough to withstand the cam-follower forces. This meant that, assuming the original design of the system was careful, the radius of the cantilevered roller bearings was a calculated value and important to be carried into the new design.

The roller radius was 1.25 inches. The bearings initially selected were specialty bearings that did not require lubrication. Between the inner and outer races of the bearing, a layer of Teflon limited the friction as they rolled against each other. These bearings, though more expensive, were desirable because the vibrational noise of roller-less bearings is significantly less. This reduced level of noise gives cleaner data output for the machine.

The Teflon roller bearing initially chosen is shown in Figure 29:



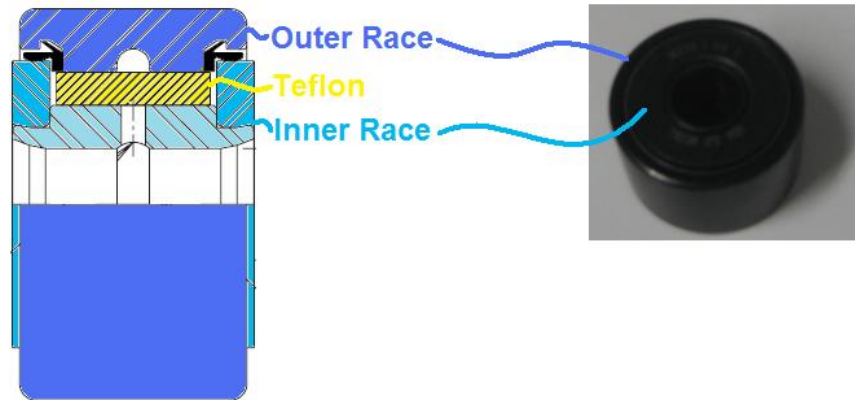


Figure 29

Note that the inner race is wider than the outer race. This is intentionally done so that the inner race can be clamped when the part is yoke (straddle) mounted. In addition, in order to ensure one instantaneous point of contact between the cam and follower rather than planar (surface) contact, the roller bearing needed to have a crowned outer race. In other words, it must have a slight curve so that the center of the roller outer surface has a greater radius than the sides. The bearings initially chosen and shown in Figure 29 are known at McGill Bearings as BCCYR and have a shaft diameter of 0.375 inches.

Ultimately, these bearings were not used; as speed of rotation increases, the ability of Teflon to withstand forces decreases. The size of the roller relative to the average radius of the cam meant that the speed of the roller was about six times that of the cam shaft. At the desired camshaft speed of 260 RPM, the roller would be spinning at approximately 1560 RPM, and at this speed the roller would only be able to withstand forces of about 20 lb. The anticipated forces at the roller were on the order of 70lb, so these Teflon bearings could not be used. Needle bearings of similar size were found to be capable of withstanding hundreds of pounds of force, which meant they could withstand the forces anticipated in the system with a factor of safety.

The dimensions and specifications of bearings are standard among bearing manufacturers and suppliers, so replacing the Teflon bearings with needle roller bearings was not difficult. The equivalent roller bearings were McGill CCYR. These needle bearings were the same size and shape as the Teflon bearings, except that the surface of their outer race was crowned. The diameter of the inner race, also known as the “clamping diameter”, was 1.075

inches. The nominal width, dictating the width of the corresponding well in the follower arm, was 0.8125 inches.

### 3.2.2 The New Follower Arms

The design of the arms was restricted by the product specifications, the design goals, the roller bearing dimensions, and the need for points of connection to various other parts of the trains. Figure 30 shows the rough concept design for these parts following the rejection of the design in the beginning of Section 3.2:

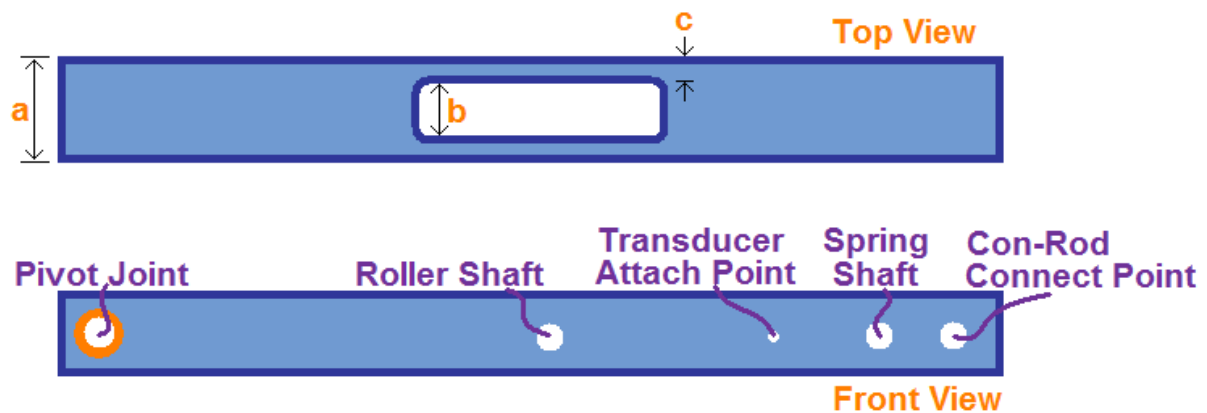


Figure 30

This concept followed the specification that the arms should straddle-mount their rollers and helped prevent the cams from contacting the arms. The arm height, similar to the original follower arm, was 1.5 inches. To ensure that the bearing would fit in the follower well, width “b” from Figure 30 was designed to be at minimum 0.813”. The nominal value of “b” was therefore 0.814”, according to the assumption of  $\pm 0.001$ ” tolerances in CNC machining. See Appendix C for specific information regarding the tolerances involved in axial spacing and the resulting nominal dimensions.

Distance “c” is half the difference between “a” and “b”, and represents the wall thickness on one side of the well. The initial value for “c” was chosen as 0.5”. Two issues existed with this design. One critical issue was that of attaching the springs and con-rods to the arm. As mentioned previously, the overall width of the arm being much greater than the original arm prohibited using connectors that would straddle the arm. The other issue was that of weight. The weight of the follower arm is correlated to the maximum force exerted in the system, so reducing the weight was another goal in the further development of the arm design.

Another concern was that, in addition to having contact between the cams and the arms in the original design, there was also harsh contact in jump between the arms and the base plate. During a normal cycle, when the cams forced either arm into its lowest position, the distance between that arm and the base plate was 0.01 inches. When the roller left the surface of the cam at high camshaft speeds (jump), this clearance was not enough for the arm to return to the cam without crashing into the base. Though the system would eventually be designed with enough spring pretension to cover the possibility of jump at the expected operating speeds, it was desirable to soften or eliminate the blow if jump occurred. The design solution was to remove a wedge-shaped piece at the back of the arm so that, when attached to the pivot, the angled surface would be level with the base.



Figure 31

With this wedge shaped cut added to the design shown in Figure 30, the new concept was used as a starting point for an iterative finite element analysis geared to determine stiffness and deformation at the con-rod end. The process was complex because the mass, the center of gravity, and the second moments of inertia for the part needed to be determined, then a spring constant and pretension for the spring entered in DYNACAM, and then the maximum force calculated in DYNACAM and translated by moment equivalence to the end of the arm. Finally, the arm was constrained and had this maximum load applied to it in ANSYS Workbench. Finally, the deformations and stresses were calculated.

To analyze the affect that weight-reducing cuts had on the stiffness of the arm, various types of cuts were applied to the base model and the resulting deformations and stress concentrations were investigated.

### 3.2.2.1 Iterative Finite Element Analysis Procedure

The initial set-up of the finite element analysis performed on the arm design concepts was done by-hand in order to validate software values. The calculations and the set-up are

explained in detail in Appendix B. This section details the procedure by which the parts were analyzed in ANSYS Workbench during each iteration:

Upon exporting the ProEngineer solid model into ANSYS Workbench, the first step was to set the unit system to match the study (English inch-lb-second). The second step was to apply a material to the part. The material applied was 6061-T6 Aluminum. The material library entry for this Aluminum alloy was used, which has values pre-entered such as the young's modulus and the poisson's ratio.

The next step was to select a style of mesh and apply it to the geometry. The method of meshing chosen was "tetrahedrons", which broke the part into individual tetrahedral elements.

The following step was the establishment of boundary conditions through the restriction of the degrees of freedom of motion of the part. In the simple hand-calculation model, it was easy to lock the displacement at the pivots because the beam was treated essentially as a 2D system. The 3D model of the part has holes for the pivot pins, and those locations were more difficult to lock down without modifying the result. In the case of the follower arm, the pivot location needed to be restricted from rotating about the x or y axis, and from translating in the x or y direction, and the roller location needed to be restricted from rotating about the x or y axis and from translating in the y direction. These restrictions on motion were achieved using remote displacements. These "supports" were applied to the internal cylindrical surfaces of the holes in the follower arm wall, and their "remote locations" were set to the central symmetric plane of the arm, centered on the axis of the pin holes.

### **3.2.2.2 Weight Reduction**

Creating more extruded cuts through the top face of the part, similar to the follower well, caused little change to the overall stiffness of the part and greatly reduced the weight of the arm. These new wells are shown in Figure 32.

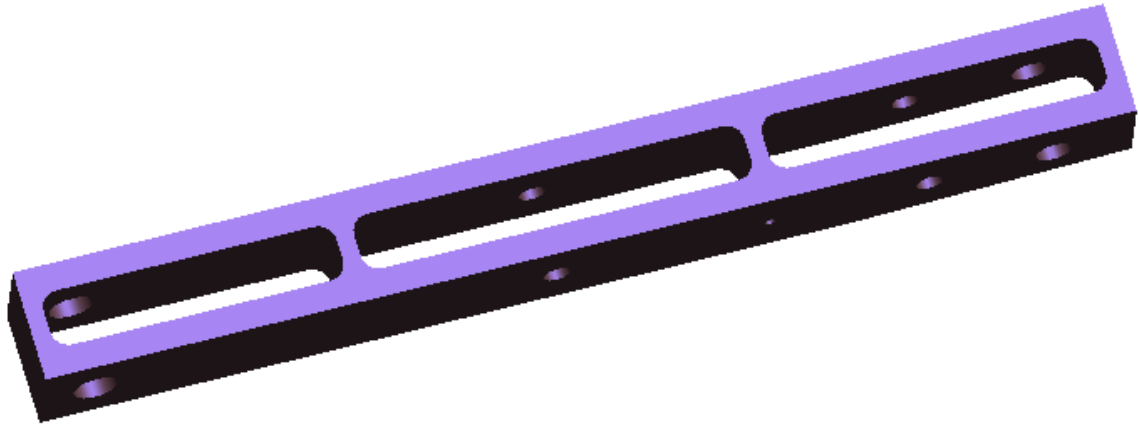


Figure 32

Making similar pockets through the horizontal faces of the part, however, significantly reduced the arm's ability to withstand its loading. With the same forces applied to the part, the deflections were twice as great and the stresses concentrated at the edge of the horizontal pockets. This is because the loading of the arm is much like a cantilever beam, fixed at one end, and pulled upward at the other. Removing material in the horizontal face was equivalent to shrinking the thickness of the beam, which in turn reduced its stiffness and increased deflection at the end where the force was applied.

The vertical wells mimicking the roller well were added to the design, and the horizontal ones were not. One full pocket the length of the part was not added because the part would have lost resistance to torsion. The horizontal ribs that held the two walls together and separated the pockets were spaced so that the cam would not be able to hit them while in contact with the roller. With the addition of the new wells, the design of the shape of the follower arm was complete.

### 3.2.2.3 Design of the Other Follower Train Elements

The other elements of the original follower trains were pin-jointed to the follower arms using shoulder bolts, which are essentially shafts with small threaded tips for fastening. All of the parts of the new train were initially designed to be attached using these bolts, which meant that parts of the arms were threaded to accept them. This initial concept was eventually forgone in favor of using shafts with snap ring grooves; the snap rings on either end of each shaft lock the shafts axially to the arms. This route entailed less threading and

complex machining of the arms, and provided a more even distribution of forces across the arms as well.

With the follower arm wells decided on, a part was needed to connect the con-rod at a pivoting joint with the arm. The new wells had the added advantage of the arm being able to straddle the connector, rather than the connector needing to straddle the arm. While the height of the part and the central top threaded hole to accept the con-rod remained true to the original part, the new connector was rounded at the base and was designed to house a bronze bushing. This way, the interaction with the shaft would be low-wear. Two Teflon washers locate the part in the well axially and reduce the friction of the connector against the internal walls of the arm. The assembly of the connector and the bushing is shown in Figure 33:

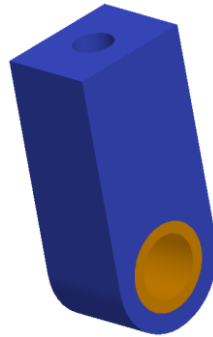


Figure 33

See Appendix C for a discussion of the width of the part according to machining tolerances.

Since the nature of the arms changed from cantilevered rollers to straddle-mounted rollers, the trains needed to be located in-line with the cams and the transducers needed to be offset. This necessitated the design of a new top block for the cam enclosure. The part remained mostly unchanged in terms of overall shape and the threads of the individual holes. The greatest deviation from the original part was that holes dedicated to the mounting of the transducers were added, as opposed to attaching them directly beneath the spring brackets. The new part is shown in Figure 34:

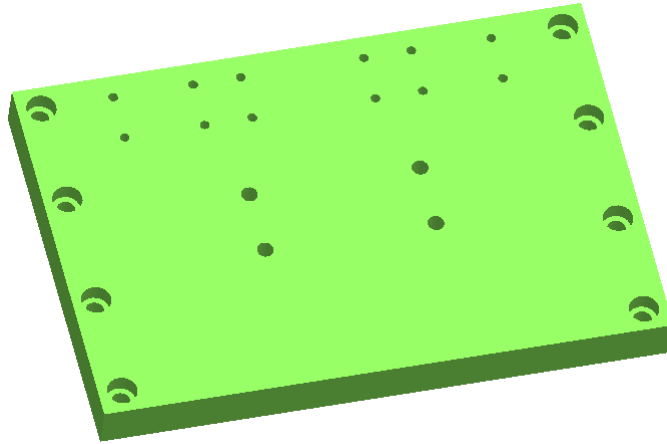


Figure 34

The change in width of the follower arm from the original design meant that a new pivot block was needed. A challenge to the design of such a part was the base plate; it is a large solid block of metal, unable to be removed from the machine, making it desirable to reuse the holes for the previous pivots, but those holes did not line up with the new arms. This mismatching of dimensions was solved by using only two of the four holes and making the pivot block one part. The holes are illustrated in Figure 35:

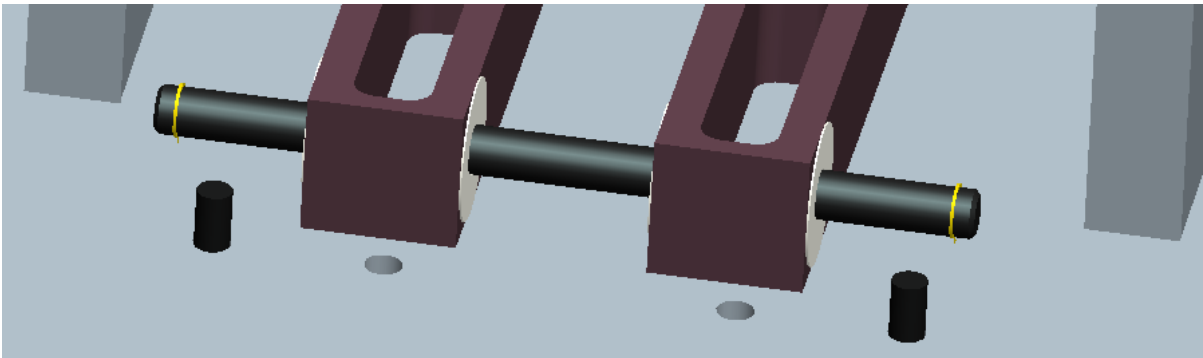


Figure 35

With the block hidden, the interference between the center two hole locations and the arms can be seen. Figure 36 shows the new pivot block.

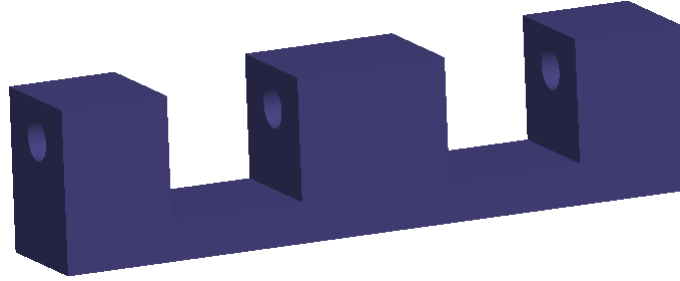


Figure 36

A critical and non-obvious aspect of the pivot block was that the holes in the block used to mount it were not symmetric about the plane that is at the center of the two cams. This meant that the distance from the left edge of the part to the first hole needed to be less than the distance from the hole on the right to the rightmost edge of the part. The centering of the block relative to the cams rather than the holes in the bearing block was critical because the pivot block locates the arms in-line with the cams and the other moving parts of the follower trains.

Research was performed on commercial devices that could replace the dangerous and torque-inducing spring pre-tensioning assembly, and the most promising result of the research was the industrial turnbuckle. An example is shown in Figure 37:



Figure 37

Turnbuckles are relatively easy to tension, predisposed to the type of attachment and use needed, and they can twist to account for the angled offset of the top and bottom hook of each spring. The selection of the proper turnbuckles for the follower trains of the CDTM was as iterative as the choice of the arm width; the turnbuckle needed to be able to be long enough to connect at first to the un-stretched spring and the follower arm, then tighten



enough to provide the right level of pretension. The turnbuckle also needed to withstand the same tension forces experienced by the springs.

### 3.2.2.4 Width Optimization

To match the product specification that the deflection of one end of the arm must not exceed 0.005 inches, and to determine a system where a real commercially available spring would match the spring constant and pretension used to satisfy DYNACAM, further and more detailed iterations were performed.

To perform a dynamic vibrational analysis and output the most accurate value for the maximum force, DYNACAM, required that the masses of the links and the stiffnesses of the parts be entered. It used those values to produce an effective mass of the follower train at the roller. The mass properties and mass moments of inertia at the centers of gravity calculated using ProE helped determine the effective mass and check it against the DYNACAM value.

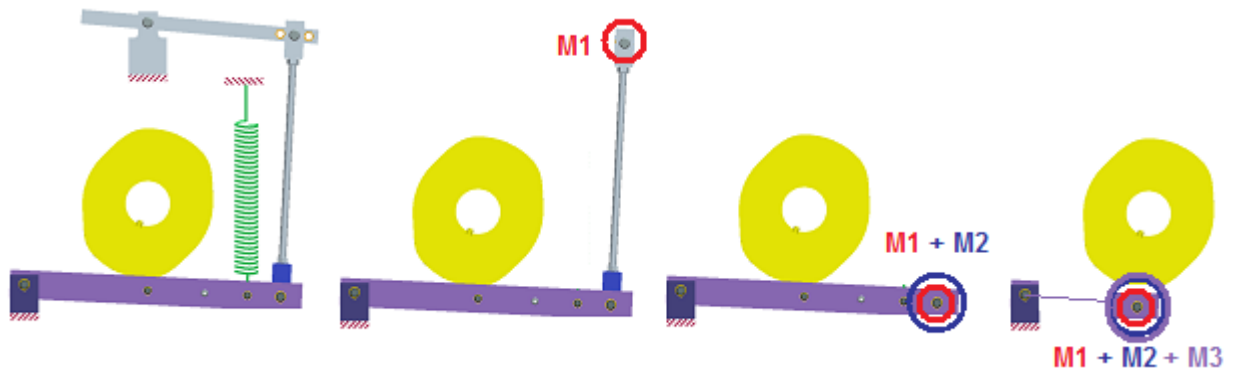


Figure 38

The width ultimately chosen for each wall of the follower arm was 0.4 inches. The maximum forces in the primary and compensating trains differed, so different spring constants and springs were chosen to complete the two trains.

An important determination was that no physical springs were available with a significant enough safety factor in tension to operate the trains properly at 285 RPM (the maximum shaft speed resulting from the motor's operation). This led to the decision to limit the speed of experimentation to 260 RPM so that a real solution could be obtained. The details of the final solution, including turnbuckle selection, are shown in Table 2:

**Table 2: The Final Design**

Property	Primary	Compensating
Arm Wall Width	.4"	.4"
Maximum Force Experienced at Spring/Turnbuckle	71.3 lb	122.25 lb
Limiting Load Boundary	108.1 lb	161.2 lb
Resulting Safety Factor	1.52	1.32
Turnbuckle	30315T611	30315T611
Spring	LE177N01 S	LE177L 02 M
Spring Initial Length	5"	5"
Preload Total	22.13 lb	41.49 lb
Initial Preload	8.259 lb	10.97 lb
Resulting Extension for Remaining Preload	.436"	.65"
Deflection	.005"	.010"
Outside Diameter	1.75"	1.5"
Spring "K"	31.82 lb/in	46.9 lb/in
Spring Extension Limit	2.623"	2.345"
Extension Safety Factor	1.963323353	1.512903226

The various parts and sub-assemblies that make up and mount the two follower trains are shown without the turnbuckles and springs in Figure 39:

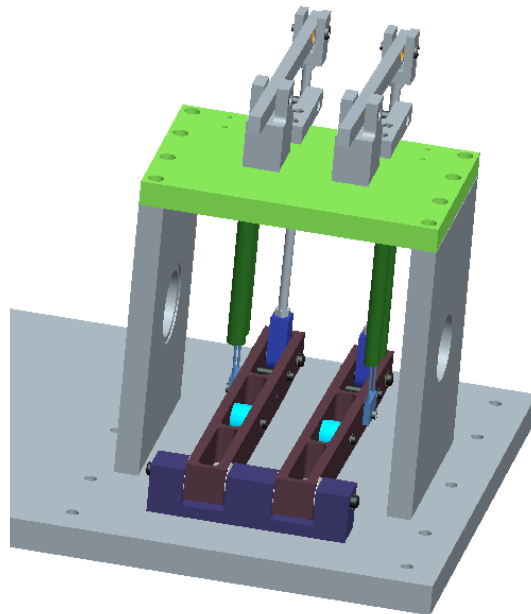


**Figure 39**

### 3.3 Improving Experimentation and Classroom-Readiness

To expand the possibilities of data collection using the CDTM to include classroom use, recording all sets of data simultaneously, and connecting with almost any computer that can use LabVIEW, research was carried out to find a DAQ or other means of data transfer that could be installed onboard.

LabVIEW is programmed to cooperate and communicate well with National Instruments equipment, making NI DAQs logical choices for use in conjunction with VIs. An original concept was to have a desktop computer installed in the lower section of the CDTM. A desktop computer would have taken up too much space, however, and would have been less easy to mount. In order to ensure that the sensors could be read with a typical external computer running LabVIEW, the solution was required to operate over USB when communicating with a computer; USB is a universal and very common data transfer protocol. A PCI to USB card adapter (MAGMA CB1H) that would allow a PCI card to be used on a laptop, shown in Figure 40, was investigated. The concept was that the adapter would allow DAQs with PCI outputs to connect more universally with laptops and other computers.



Figure 40

An issue with this solution was that laptop manufacturers are in a transition period, switching from PCMCIA to PC Express cards. Some manufacturers are removing the standard completely from their laptop lines as there are fewer and fewer peripherals that require a high-speed data pipeline that can't already be accommodated by USB or Firewire.

National Instruments strongly recommended against using MAGMA converting devices as they have had situations where LabVIEW would not correctly recognize DAQs or they would inexplicably stop sending information to a computer. NI also mentioned that they do not provide any technical support to troubleshoot any communication problems when connected with the MAGMA CB1H. The final problem with this approach was the \$1000 cost.

Two more expensive NI devices had USB outputs, avoiding the need for a MAGMA adapter; NI USB-6210 is shown in Figure 41 and the USB-6229 BNC is shown in Figure 41:



Figure 41



Figure 42

In addition to being the most common data transfer protocol (next to Ethernet cable), the USB standard is also backwards compatible. USB 2.0 devices will still be able to run at full speed on USB 3.0 when that is the standard.

Both the USB-6210 and the USB-6229 BNC were capable of sampling at 250,000 samples per second, and offered digital inputs and outputs (48 on the 6229 and 4 on the 6210) which would allow connection to a frequency inverter. The 6229 had 4 analog outputs that could output or amplify data. The USB-6210 was almost a fourth of the cost of the USB-6229 BNC. The 6229, however, had BNC inputs so that all cables could maintain signal integrity while allowing tool-less replacement of cables and connection of auxiliary sensors to the DAQ. The benefits of utilizing the 6229 and the potential to expand its use outweighed the difference in cost, and that was the DAQ chosen to be dedicated to the CDTM.

### 3.3.1 Creating the Virtual Instrument

The Virtual Instrument was designed to read all 10 output channels of the CDTM simultaneously, to write data to spreadsheet, and to provide graphical displays of the data collected.

The front panel, serving as the control and display part of the VI, is shown in Figure 43:

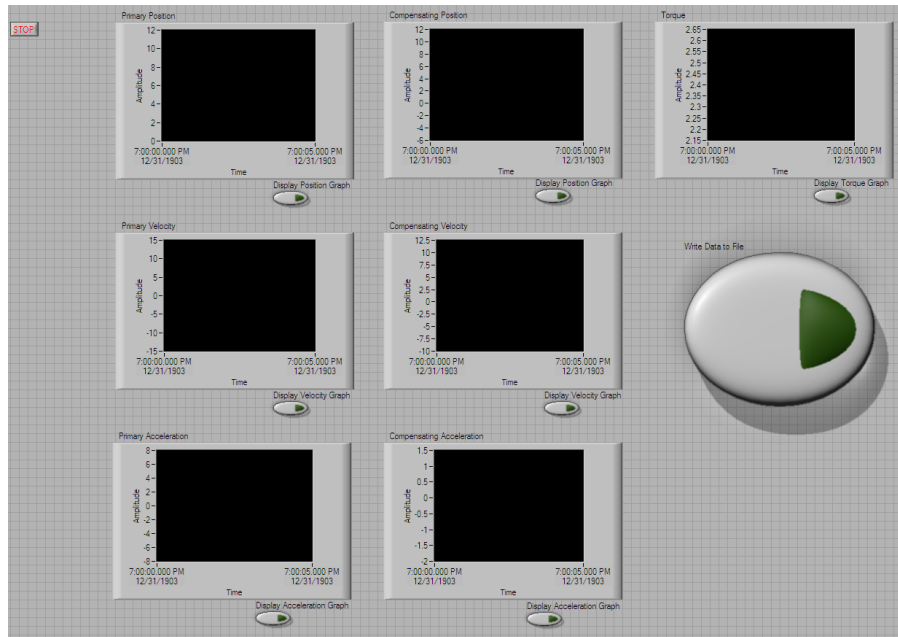


Figure 43

The seven chart regions display data real-time as it is collected. They correspond to all the sensors except the encoders (because their data is binary and uninteresting for display purposes).

The block diagram of the VI, which is the graphically-coded definition of the function of the VI, is shown in Figure 44:

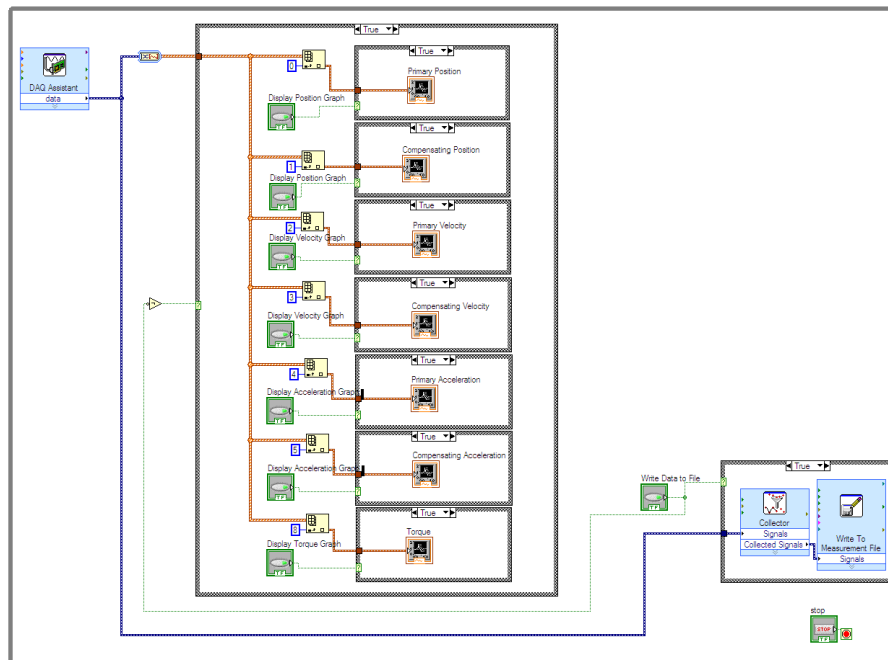


Figure 44

The block diagrams first element, on the upper left, is the DAQ Assistant, which was programmed to recognize the DAQ from the USB signal connected to the computer. The DAQ Assistant recognized the specific lines of data coming from each of the sensors. The central “true-false” loop was designed to split the large combined stream of data into its individual elements, and to display that data on the charts of the front panel. The combined data stream was also run to the “true-false” loop on the lower right. The two elements in this loop, used in conjunction, allow the data to be recorded while streaming and permit meaningful and fast writing of the data to spreadsheet.

The VI accompanies this report electronically, and is open to further development.

### **3.3.2 Operability in Classrooms**

The original motor of the CDTM could be run from a 120V AC wall outlet, and could thus be demonstrated in lecture halls. Since this important capability was lost when the current motor and power cable were installed, a goal was to find a way to power the new motor in classrooms.

The possibility of connecting two separate cables to 110V power outlets on separate circuit breakers, each capable of putting out 20A, was investigated. For this to power the motor, a step-up voltage transformer would effectively give 220V single phase at 20A which could then be converted to three-phase power by the inverter. This design was contingent on such power outlets existing in the same room, which was difficult to determine and generally rare.

A meeting with one of the Campus Electricians revealed that this type of configuration, while possible, is generally unsafe and is strictly a violation of electrical code. The electrician revealed the location of spare three-phase power lines that could be used for the project, and mentioned the possibility of running lines to specific classrooms. Fortunately, a source of three-phase power existed already in one of the large lecture halls.

The caveat to using that power outlet was that the connector did not match the one on the machine. The plan was to remove the current connector, replace it with a male connector matching the wall outlet, and to also build a cable with a female end matching the wall and a male end matching the lab power outlets, so that the machine could operate in both locations.



### *3.4 Improving the Electrical and Storage Configurations*

As described in Section 2.2, there was room for improvement in terms of both the wiring and the use of space within the frame of the CDTM. Long wires were strewn about and connections were either wrapped in electrical tape or left exposed. The front panel BNC connectors were weakly connected to the data cables, and the power supplies were inadequate and unprotected. The large new motor controller was left on the low plastic shelf in the base of the machine because it could not be more conveniently mounted in place of the old one in the front panel, making it difficult to access and use. The aim was to maximize the utility of the space within the lower half of the machine, mount all the parts that were lying in the bottom at the outset, and rewire power and data to connect to the DAQ and to organize the wire mounting within the frame.

#### **3.4.1 The New Mounting and Storage Plan**

In addition to the parts dedicated to the functioning of the machine, such as the motor controller, the power supplies, the motor, and the wires, there are many other parts that are related to the machine, such as alternative follower trains and spare screws. In an effort to organize the underside of the machine, to mount all of the necessary parts, and to provide on-board space to store associated parts and tools, brainstorming was carried out on a new layout for the space.

The layout plan was restricted by the location of the motor and the moving belt, and by the screw-down bolts that connect to the four jack feet of the machine. Figure 45 shows the original shelf and the space available.

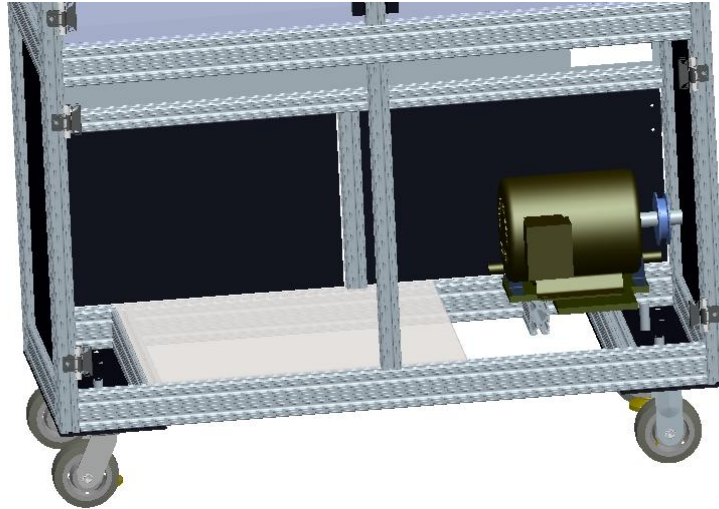


Figure 45

The design concept for the redesign of the space called for shelves, drawers, and mounting for the major components. The feasibility of the realization of the design was the primary concern, and using 80/20's proprietary bars and connectors was found to be an effective way of connecting to the frame. The basic concept of connecting to 80/20 bars is illustrated in Figure 46:



Figure 46

The green exterior part is held to the surface of the 80/20 by putting a screw through it which then grabs the threads of a slot-fitting connector (blue) that sits inside the profile's groove. Two types of threaded slot-fitting connectors are sold; the less expensive ones can be slid into the grooves prior to a bar's installation, whereas the more expensive ones can be slid into the groove even if the bar is already installed. The more expensive connectors were needed so that the existing frame bars could be used to support the new frame elements.

The original frame was assembled by drilling and tapping holes in the bars, then inserting screws through one bar and into another. The drilling and tapping were accomplished while the pieces were separate. In the case of adding more frame elements to support drawers, shelves, and mounting of equipment, the luxury of drilling new holes in the

original frame was restricted by the difficulty of disassembling the machine. Using the old method of attachment would involve either taking apart the whole machine or using a hand-drill; neither course was particularly desirable.

An alternative to those methods was to use proprietary brackets and plates in conjunction with the slot-fitting connectors described above to attach new pieces to the existing frame. Some of these brackets and plates are shown in Figure 47:

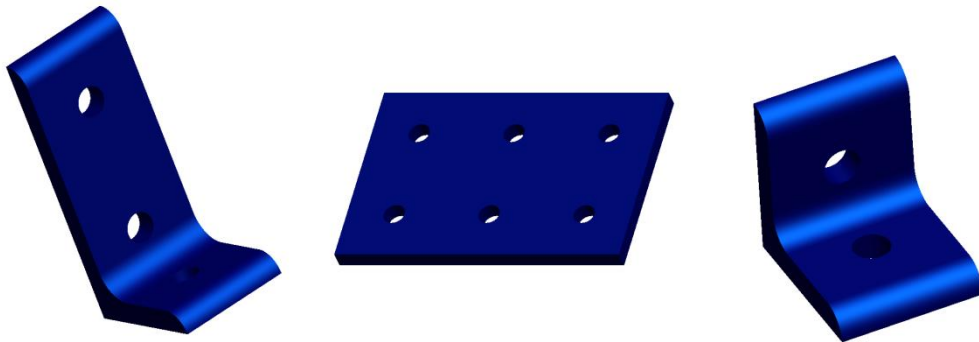


Figure 47

Another benefit to framing the new layout with 80/20 was that there were different extruded profiles that could be used together; the type most typical of the existing frame was twice as long as it was wide, but there were also square profiles and half-width profiles in the same family to work with.

To add a shelf that would run almost the whole length of the machine, the horizontal bar on the front at the base of the front panel was mimicked at the backside with two square bars at the same height, as shown in Figure 48:

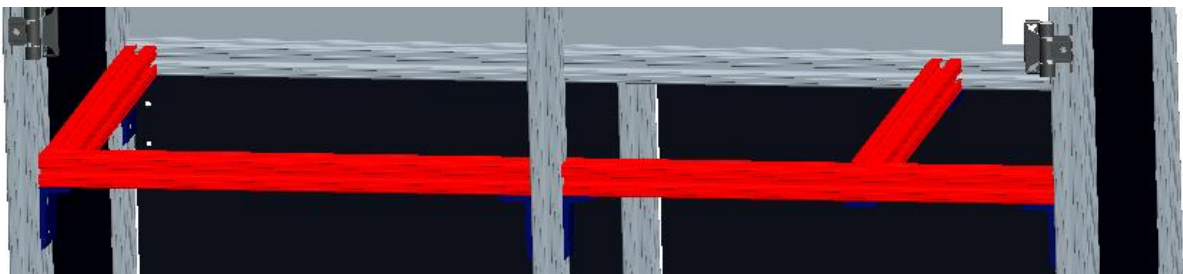


Figure 48

Also shown are the cross members added to form the ends of the shelf. In the figure, the rightmost (on the flywheel side of the machine) was inset from the edge of the frame to allow room for the belt.

The shelf is made of 1/8" sheet metal, about 20" by 36", and was designed to rest in the grooves of the two end pieces. To support the shelf, half-height 80/20 bars with one flat side were added intermittently and attached with plates to the outer bars, as shown in Figure 49:



Figure 49

Note that in the center of the frame, rather than using a flat bar to support the shelf, a larger cross-sectioned bar was used; this was to make it useful in the next steps of the design, adding drawers and mounting the equipment.

To add sliding drawers, slide rails were researched. 80/20 reported that while they did not fabricate drawer slides, McMaster Carr offered slide rails that were frequently used in conjunction with 80/20 frames. 20" (closed) McMaster Carr drawer slides were a good match to fit within the length of one side of the CDTM frame. The original concept for adding drawers involved the addition of twelve 20" double-wide 80/20 bars; four were to be used to frame each drawer and four more to mount the rails. This design is illustrated in Figure 50:

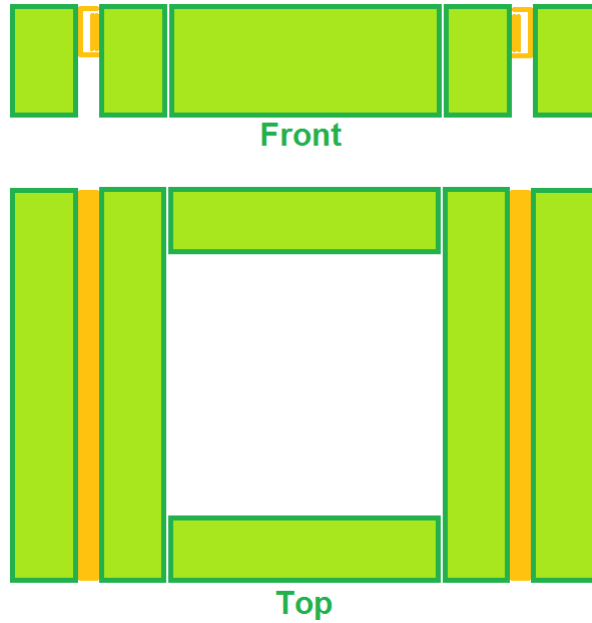


Figure 50

The outermost bars were to be mounted to the frame. This original concept, however, overused the double-wide 80/20 bars, making the drawers heavier and the mounting of the rails more cumbersome. The cross-bars in the frame of the drawers were modified to be half-width, and the rail mounting bars were changed to be square bars. These changes are shown in Figure 51:

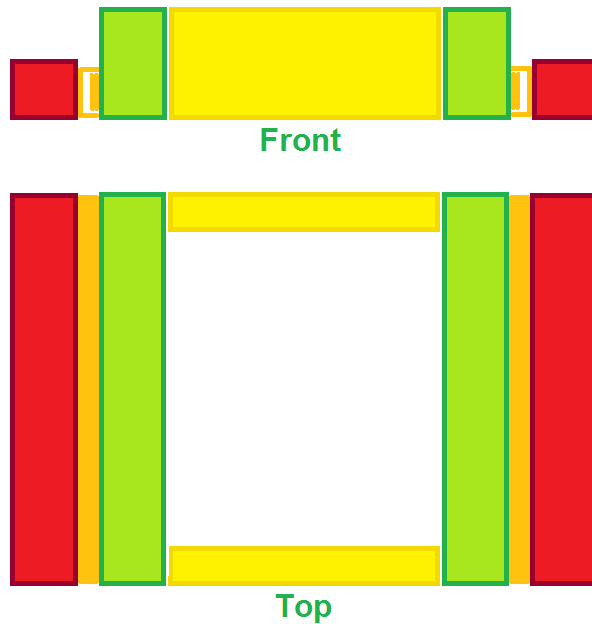
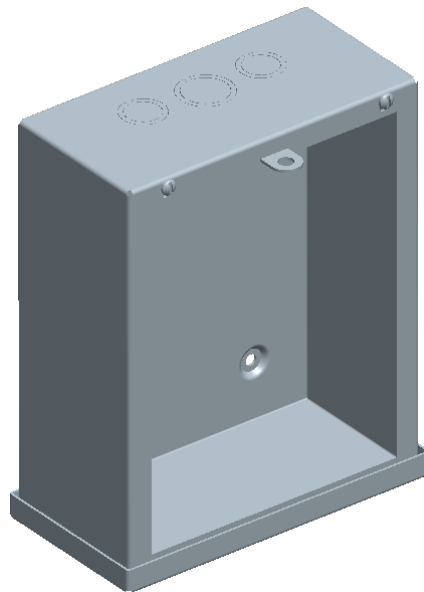


Figure 51

To complete the design of the drawers, a way to fasten the four drawer-framing bars of each drawer was researched, as well as a way to support the sheet metal at the base. Originally, the sheet metal was to be put in the bottom groove of the 80/20 framing bars, but this wasted some of the height of the bars that could have been used as drawer depth. Also, the plan was to support the sheet metal in a similar fashion to the shelf, with half-height bars fastened with plates to the bottom side of each drawer. These cross bars added weight, however; in this case, trying to make use of the 80/20 grooves to attach and secure the drawer bottoms was not the most effective route. Instead, the sheet metal was planned to have through holes drilled in it, and then tapped holes would be added to the bottom of the drawer frame, so that the drawer bottoms could be attached by screws.

Since the drawers were planned to span the space between the center bars and the side of the CDTM away from the motor, the motor side was reserved for mounting the DAQ, the power supplies, an AC power block, and the motor controller. Earlier troubles with the exposure of the power supplies led to the conclusion that they should be enclosed within the CDTM. Rather than construct an enclosure, typical electrical enclosures were researched. The chosen power supply enclosure is shown with the front cover removed in Figure 52:



**Figure 52**

The three circular shapes on the top were removable and intended to pass cables into and out of the box. The four holes in the back were for mounting using screws and washers. To avoid connecting the box to the frame electrically, the design called for nylon screws and rubber

grommets to be used to connect the box to the frame. The supplies would be mounted with stand-offs to the walls of the box.

Similar to the enclosure, the DAQ had a four-screw mounting strategy. Since the data cables that needed to run to the DAQ came from the T-stops on the front panel (described in Section 3.4.2), the design located the DAQ towards the front of the machine. The power enclosure was planned to be mounted next to the DAQ but in the back of the machine. The original plan for the attachment of the DAQ and the enclosure involved putting two cross bars in the center of the frame, one at the height of the top set of screws for each, and one at the height of the bottom set of screws. The lower bar would have also served as the height of one of the drawers. This design restricted the bars to be at the exact heights of the screws and the drawer placement did not permit an optimal use of the space. The design was modified to include four vertical bars that would be located in line with the screw holes on the devices. The two cross bars could then be placed to optimize the drawer placement so that the lower drawer had the most height while still allowing room for a shallower upper drawer. Figure 53 and Figure 54 show the layout of the DAQ, the enclosure, and the bars meant to hold them.

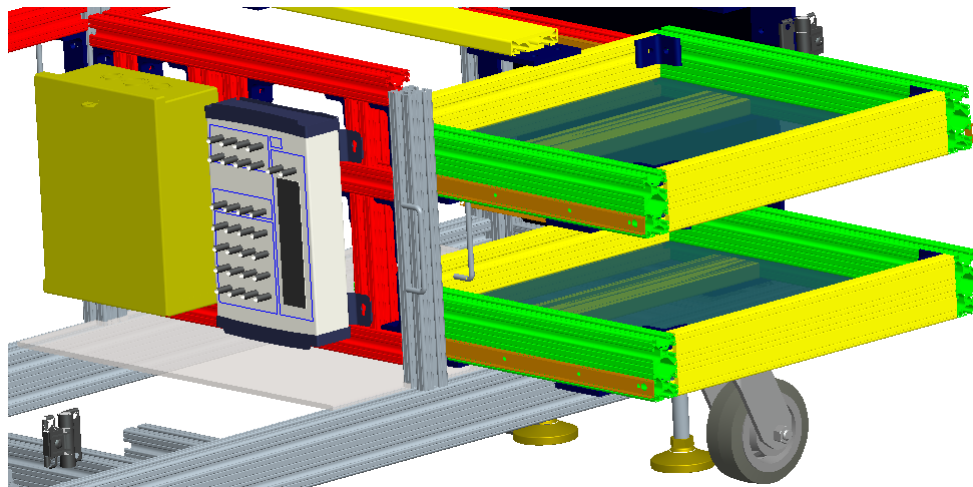


Figure 53

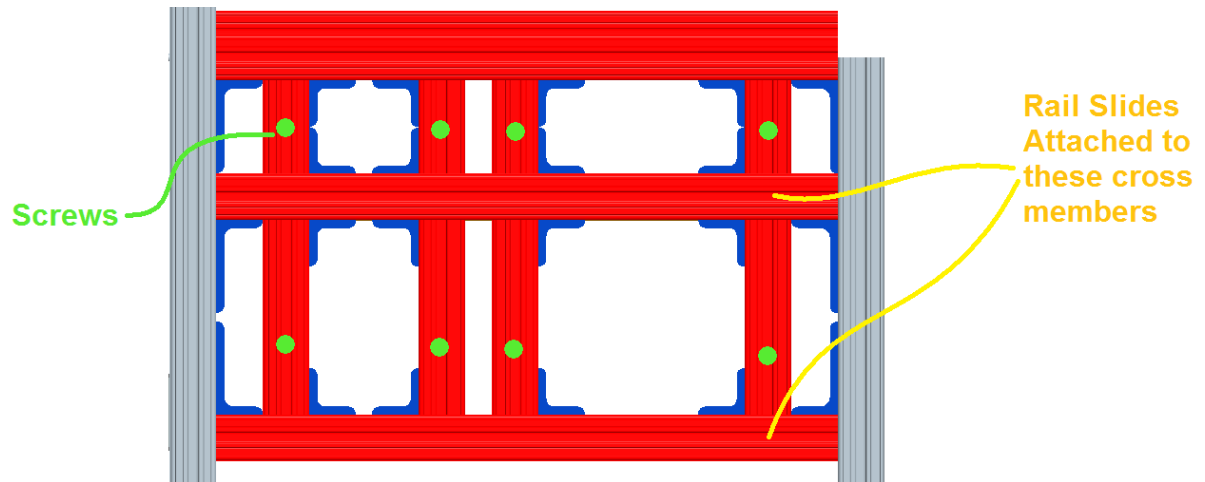


Figure 54

To completely mount the drawers, matching bars were added to the design opposite the two shown in Figure 54.

The motor controller, in this case a frequency inverter from AC Technology, was difficult to mount due to its size and the location of its screw holes at the four corners of the heat sink that extrudes from the back. The first step towards mounting it was to build a frame of 80/20 bars that it could attach to. This frame could then be attached to the frame of the machine. There was just enough space next to the motor to mount the controller and allow the cables to exit its bottom. The mounting design is shown in Figure 55:

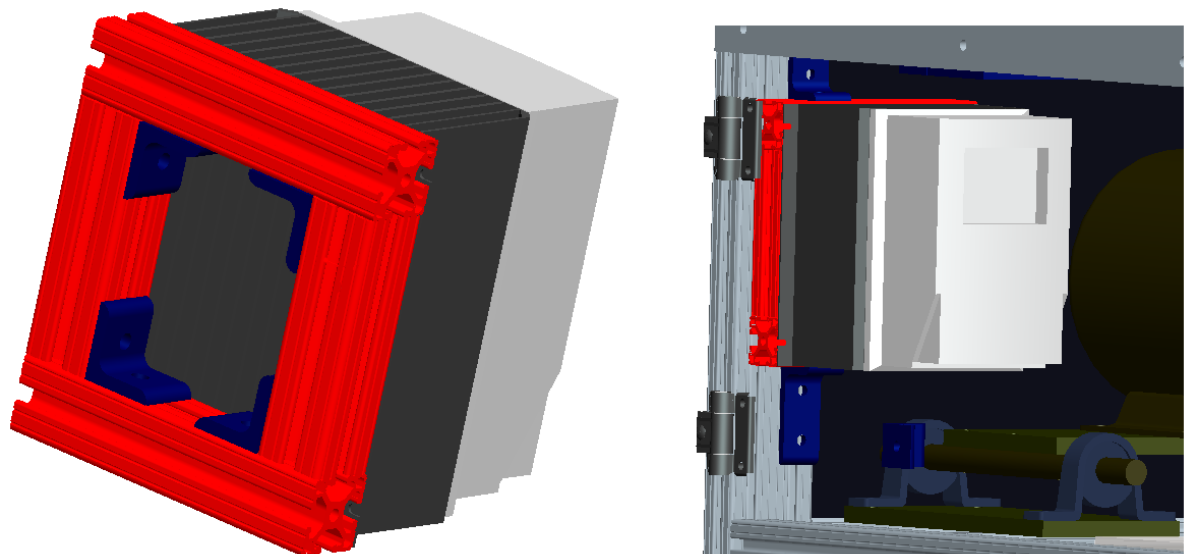


Figure 55



With this mounting concept complete, the design of the new additions to the lower half of the machine was complete. The complete model of these parts all installed is shown below, with the front panel and the opaque doors and sides hidden:

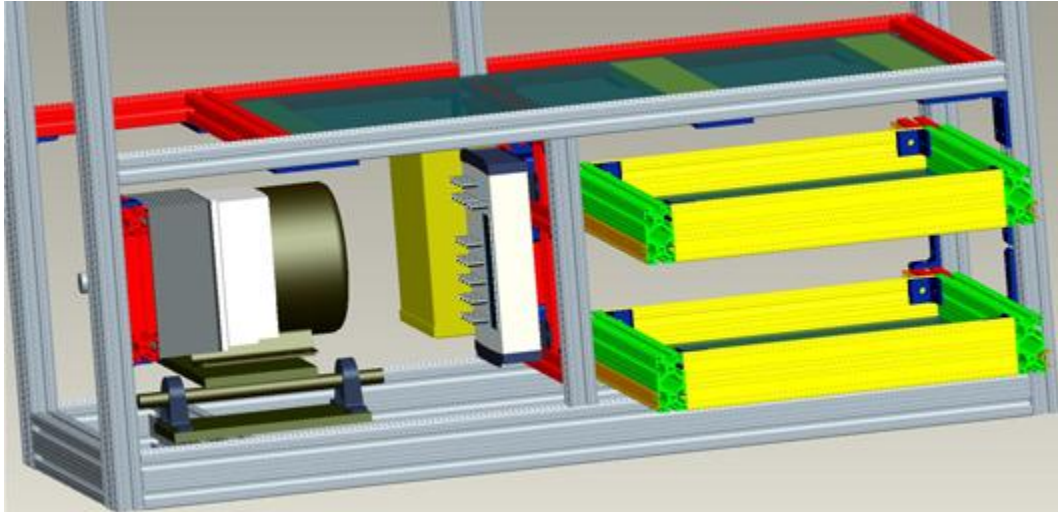


Figure 56

The new frame elements and drawers were very near the front edge of the machine. When the doors on the CDTM were first installed, the hinges were mounted flush with the frame, preventing them from being closed fully. This problem was exacerbated by the proximity of the new frame elements; to allow the doors to close flush without interference, a new plastic part was designed to match the hinge in color shape and dimensions in order to stand it out the same width as the doors from the frame. The new part, made of black acrylic, is shown in Figure 57.



Figure 57

Using these plastic shims required new, longer screws be purchased to fit through both the hinge and the shim and into the 80/20 groove.

### 3.4.2 The New Wiring Configuration Plan

While researching the power needs of the machine's sensing equipment, it was determined that the power supplies in use were inadequate and that the power wiring

configuration was incorrect. Table 3 shows which devices were connected to which power supply, and indicates in bold those connections that did not match a device's needs.

**Table 3: The Original Power Configuration**

Device	Need(s)	<i>Standard Power Power Supply (SPS 30DA 5/12)</i>	<i>Meanwell Power Supply (S-150-12)</i>
Optical Encoder 1	5V - 15V DC	5V DC	-
Optical Encoder 2	5V - 15V DC	5V DC	-
LVDT 1	±15V DC	-	<b>12V DC</b>
LVDT 2	±15V DC	-	<b>12V DC</b>
Torque Transducer	9V - 12V DC	<b>13.6V DC</b>	-

In this initial power configuration, three of the five sensors that required power to function were wired to receive the wrong voltages. The options for new power supplies and combinations of power supplies were then investigated; the limiting factor in the search was the need for positive and negative 15V in tandem to properly operate the LVDTs. The Meanwell T-40C, shown in Figure 58, was capable of providing this power.



**Figure 58**

In addition, the T-40C was also able put out 5V, making it a candidate for the solution. The T-40C would replace the Standard Power supply in the power circuit. Table 4 shows the connections of the devices to the old and new Meanwell power supplies, accounting for the needs of all of the sensors.

**Table 4: The New Power Configuration**

Device	Need(s)	Meanwell Power Supply (S-150-12)	Meanwell Power Supply (T-40Ca)
Optical Encoder 1	5V - 15V DC	-	5V
Optical Encoder 2	5V - 15V DC	-	5V
LVDT 1	±15V DC	-	±15V DC
LVDT 2	±15V DC	-	±15V DC
Torque Transducer	9V - 12V DC	12V	-

Once the power requirements for the sensors were accounted for, the wired connections between the sensors, power supplies, and DAQ were designed. There were three parts to this design challenge: researching the best suited cables for data and power transmission, determining the most applicable terminating connectors for compatibility with the DAQ and the front panel, and developing a wiring layout to optimize organization and minimize interference from the frequency inverter and motor.

Two types of cable were decided on. The cables chosen to carry power were Belden 8762 shielded twisted pair audio cables. These were ideal for power as the two conductors were twisted together to reduce AC interference before being shielded. The exposed wires within this cable are shown in Figure 59. The voltage limit for the wire was 300V, which is greater than it would supply in use in the CDTM.

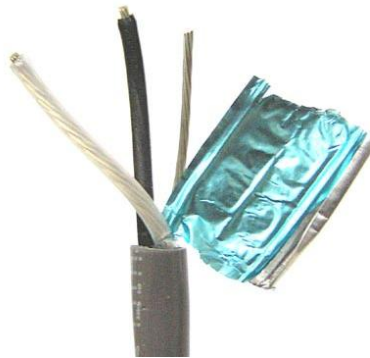


**Figure 59**

The selection of the data cable was more restricted by the specific need to support BNC connectors. RG-58, RG-59, RG-6 were all considered at first, but the outer diameter of these cables are about 0.2-0.27 inches. With ten data lines to run, the volume of cable would have

been difficult to run and organize within the frame. Belden 8216 RG-174 (also known as micro coax) was chosen instead because its outer diameter is 0.11” (Figure 60).



Figure 60

These cables are much more flexible, and their narrow profiles allow more cables to be used in the same space as the former RG Coaxial cables used. The center conductor carries the output voltage while the shield could be used as the output common for the sensors. An output common is necessary for a BNC to function correctly. When testing voltage with a digital multimeter, there are two probes to read the voltage difference. In a BNC cable, the shield acts as the common while the +V output is run down the center conductor. This allows for a voltage difference to be read with one cable, and is standard on all BNC reading devices. To avoid this shield acting as an antenna of interference, the power supplies have their DC V0 earth grounded. This means that whatever interference is picked up will be brought out of the machine and transferred through the building’s earth ground.

The next consideration was connecting the wires to one another as well as their respective devices. Previously, the BNC connectors installed on the front panel (except for the accelerometer ports) were soldered connections where regular wire was used and the conductors were soldered on. While this is common practice, it opened up possibilities for shorting the sensors’ outputs. Therefore all BNC port holes were re-drilled on the front panel to 0.5” in diameter to accommodate new male-to-male BNC panel mounted couplings, shown in Figure 61.



Figure 61

Instead of soldering, a physical connection can be made with these connectors. The connections were designed to be made through a Male-Female-Male T coupler (Figure 62)

that took an input from one side, connected to the front panel in the middle, and allowed an output that could be directed to the DAQ.

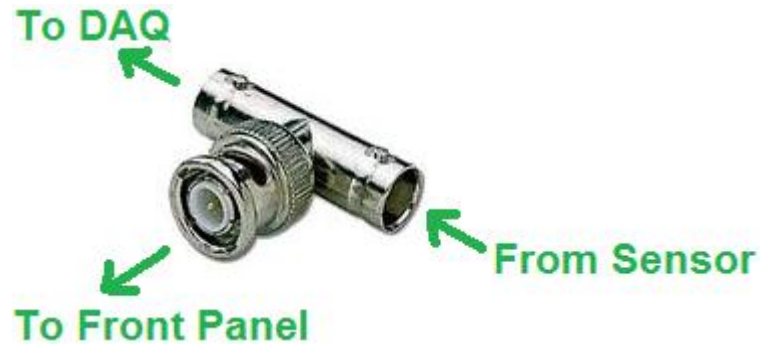


Figure 62

These connectors allowed for the front panel to be accessible while still maintaining full functionality with the DAQ. Another added benefit to these T connectors was that they were capable of being rotated; this allowed the cables to run parallel with the front panel instead of extending into the shelf area.

RG 174 BNC (Figure 63) crimped female connectors were chosen to terminate the other end of the sensor cable that connected to the Ts. They were also used for both ends of the cables used for connecting the front panel to the DAQ.



Figure 63

The data cable layout was designed to minimize the length of cable to keep signal loss low and reduce unnecessary electrical interference exposure. As soon as the wires from each of the sensors dropped below the base plate, power and data wires were split off and sent in opposite directions. Power cables were run to the rear of the machine and then run from left to right (facing the front), dropped below the shelf and then sent from right to left into the power supply housing. All data cables were run towards the front of the CDTM, where they ran from right to left and then down to the DAQ. The greatest lengths of these cables were run above the top shelf to minimize close exposure to the frequency inverter and electric motor.

### 3.4.3 The New Motor Control and Input-Output Panel

Mounting the motor controller within the frame and running the data cables to the DAQ helped organize the CDTM and make it more useful. However, there was still no easy way to access the USB data line coming out of the DAQ or to reach the controller in order to turn the motor on or off. There was also no simple way to add extra sensors in the future to expand the data collection with the machine. Also, the front panel still had a large rectangular space in it which was meant to house the original motor controller. To solve these issues, methods of controlling the motor without using the buttons on the frequency drive were researched, along with a USB panel-mounting connector. The solutions could then be mounted in the gap in the front panel on a new plate.

It was found that AC Technology, the company that produced the motor controller, offered a proprietary “remote controller” which imitated the buttons on the inverter itself. This remote control unit was only 2.0” by 3.5” by 0.5”, making it able to be mounted on the front panel with room to spare. The remote was not wireless, but the wire that connected it to the inverter was small and extended from the backside of the remote, which came with two mounting screws. The remote is shown in Figure 64.



Figure 64

Another important find was a USB B female to USB A female adapter. This device can accept either USB A or B as an input, and output the other. An accompanying part made by Neutrik is a special dust cover which the adapter fits into. The cover has holes for mounting the adapter to a panel. This way, the side that is the line-out to a computer is protected by the dust cover, and the other side extends freely through a hole in the panel it

can be mounted to so that the wire from the internal device can be connected to it. The adapter and dust cover are shown in Figure 65:



Figure 65

To make the USB line-out of the DAQ, the remote controller, and the unused inputs on the DAQ accessible despite their locations within the underside of the CDTM, a specialized plate was designed. This plate concept had holes drilled in it for mounting BNC connectors similar to those on the front panel, along with the USB adapter and the remote control. The plate design with and without the components attached to it is shown in Figure 66:

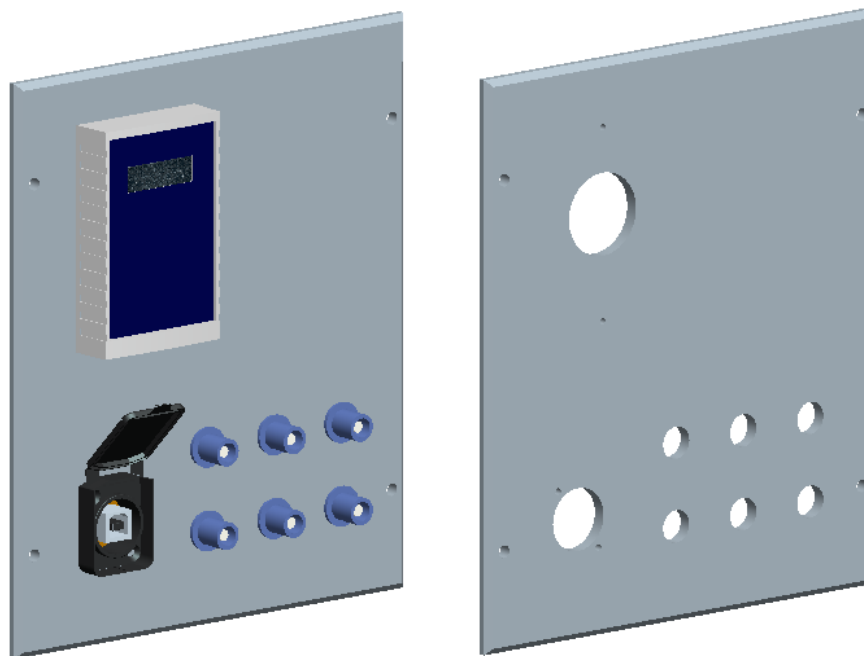


Figure 66

The four screws in the corners of the plate match the through holes used on the front panel to mount the old motor controller. The plate was designed to be larger than the space left by the old controller to cover the gap.

The plan was to run six cables from the DAQ inputs and outputs to the BNC connectors on this plate. Then, a USB cable with a B-male end to connect to the DAQ and a USB A-female end to connect to the adapter would be attached. A longer version of the same cable would be kept in a drawer and plugged into the front of the adapter and into a computer used to read the data from the DAQ.



## 4. Realization and Results

The many newly designed parts of the follower train were manufactured. In each case, stock aluminum larger than the eventual part was faced on all sides to ensure that all angles were square. The parts were then faced, milled, drilled and tapped to give them specific dimensions and features. As shown in Figure 67, plastic tubes were cut and used as spacers to locate the turnbuckles in the center of the shafts on the follower arms.

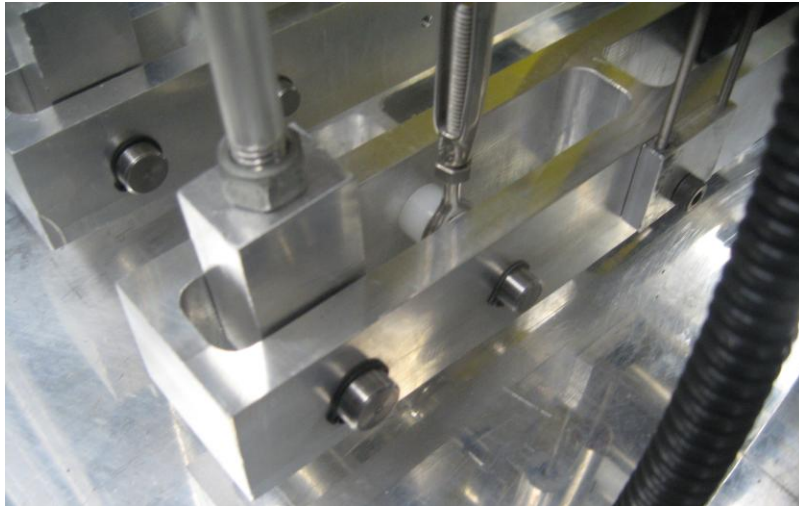


Figure 67

The shafts, such as those shown in Figure 65, were cut to length on a lathe and had snap ring grooves cut in them. The ends were chamfered to fit them into their holes on the follower arm. All holes were made one thousandth of an inch smaller than the shaft, creating an interference fit.

The bushings in the con-rod connector and in the follower arms were pressed in; the dimensions of the holes they fit into were purposefully held smaller than the outer diameter of the bushings. Once the bushings were pressed in, they were reamed to be one thousandth larger in diameter than the shafts passing through them.

The top plate is shown in Figure 68. This plate had numerous critical dimensions, mainly because it served to mount the follower trains in-line with the cams. The top plate was manufactured with a CNC mini mill using toolpaths based on the solid part model.

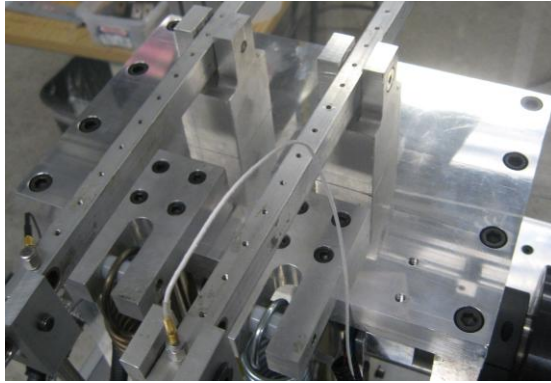


Figure 68

All of the joints were shimmed to avoid axial slop. Some of the original shoulder screws were used to join the con rods to the upper arms because that interaction remained unchanged.

Figure 69 shows the completely assembled follower trains. Note that the springs were of different stiffness to match the differing forces in the primary and compensating trains.

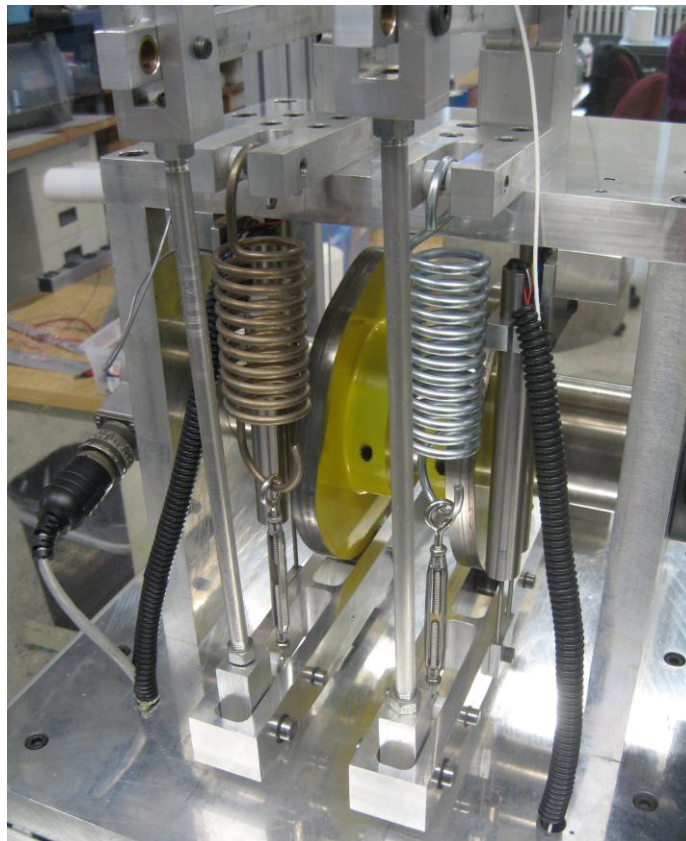


Figure 69

The alignment of the majority of the parts was consistent with the model. The pivot block, however, was more of a challenge.

The pivot block, shown in Figure 70, was difficult to machine because of the long, critical pivot shaft hole that runs the length of the part.

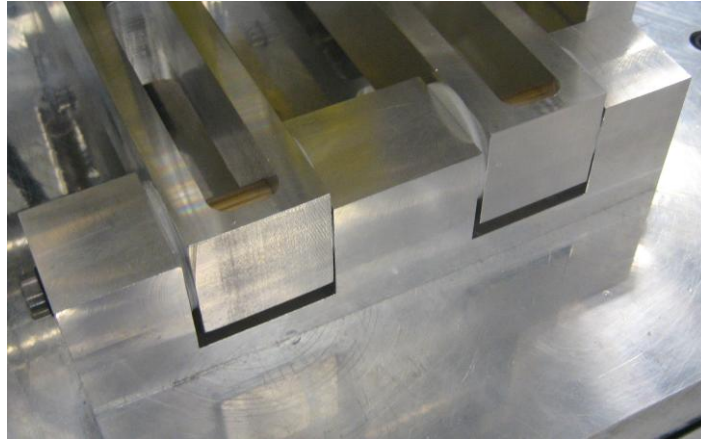


Figure 70

Though the part was machined to the specifications of the design drawing, the wells in the pivot block were not centered on the cams. This means that the CAD model was constructed incorrectly. The solution to this error was to face three hundredths of an inch from the right side of each pocket, and use a greater number of Teflon washers and steel shims to fill the wider gaps between the follower arms and the walls of the wells.

The reorganization of the underside of the CDTM added functional drawers for storage and a machine-length shelf at mid-height, behind the front panel. When making the drawers, eighth-inch metal sheets had 20 holes drilled in them near their edges, corresponding with the grooves of the full widths of the parts and the tapped holes in the half-widths. In addition to the metal bases, all the internal 80/20 grooves were filled in with special plastic gap-filling plastic. The completed drawer set-up with the lower drawer extended is shown in Figure 71:

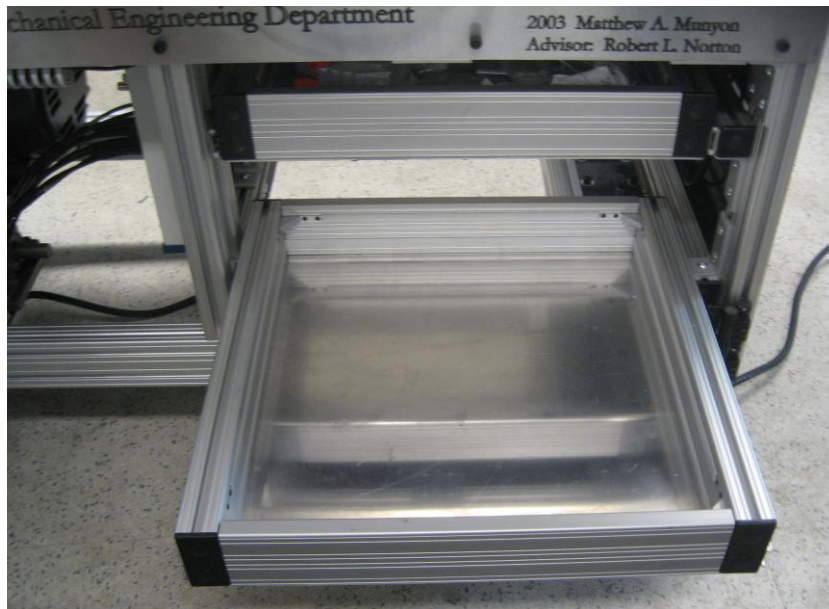


Figure 71

The internal shelf provided even more room for storage. The completed frame and shelf are shown in Figure 72:



Figure 72

As designed, the power and data cables were run in opposite directions once they were below the level of the base plate. The data cables were run along looms such as those in Figure 70 towards the front panel BNC t-connectors. The new frame pieces that supported the shelf were also useful in guiding the power cables along the back of the CDTM to the power supply enclosure.





Figure 73

Figure 71 shows the power supplies mounted within the new enclosure. To mount them, small stand-offs were attached at various threaded locations along their cases. Then, corresponding holes were drilled in the frame of the enclosure, and small screws and washers were attached to the stand-offs through the holes. The enclosure itself was mounted using Nylon insulating screws.



Figure 74

The NI DAQ was mounted next to the enclosure on the new middle frame. Wires from the t-connectors on the front panel were then run through looms and connected to the inputs on the DAQ.

Underneath, the power block responsible for providing power to the power supplies, the DAQ, and the current supply was mounted to the frame (Figure 75).



Figure 75

## 4.1 Wiring of the Sensors

The realization of both power wiring and data wiring were accomplished to provide increased safety to prevent potential shock from low voltage power. Aside from the physical installation in the CDTM, the most important step to ensure proper wiring was to use a wiring schematic (Figure 76). As the figure shows, sensor manufactures do not share color codes, so making sure that the right wires are attached to the right leads on the CDTM is essential. Assuming the same color wires for all sensors could lead to a short in the power supply and or sensor itself.

0V Common and +V sensor out were connected to the Belden RG 174 cable using the cable's shield and center conductor respectively. On the power side, the Belden Two conductor twisted/shielded wire's black and white conductors were attached to the positive voltage and common ground of the sensor. There was one exception where the shield was used on the two conductor cable with the LVDT in which the the black was associated with -15V on the LVDT and the white conductor was associated with the +15V on the LVDT.

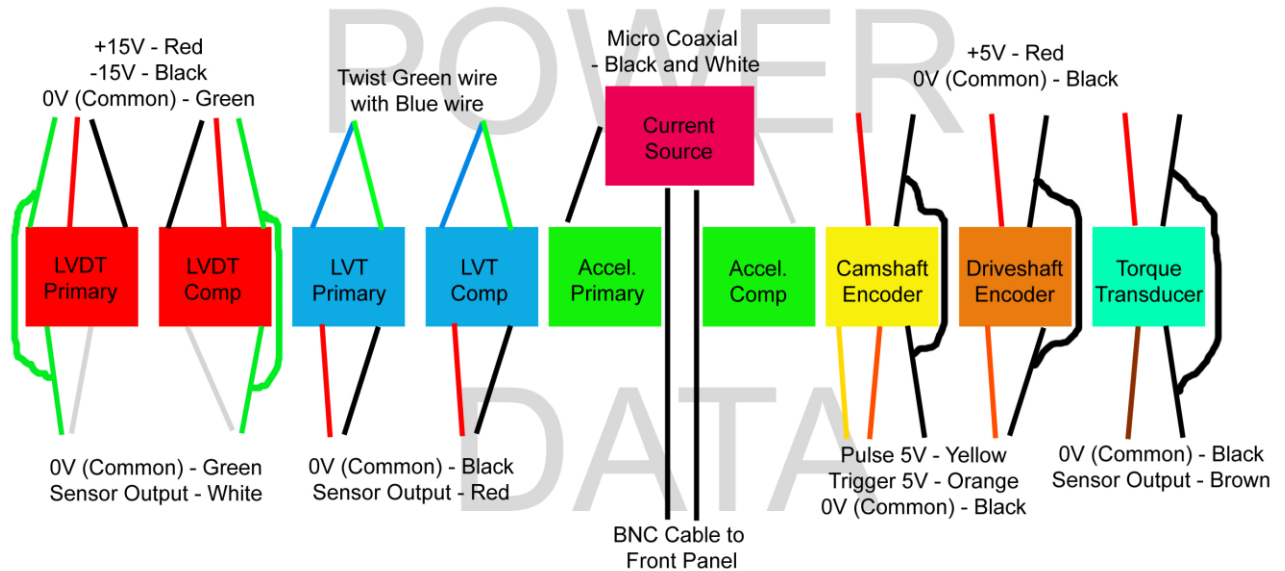


Figure 76

At the DAQ and Front Panel, BNC connectors were soldered onto the ends of the cables and the connections were sealed with heat-shrink tubing. At the sensor ends of the cables, the sensor wire was cut to a length that allowed for further re-termination if necessary. The outer cables were stripped back about an inch and a half, and the individual

conducting wires were separated. Those conductors were then soldered and heat shrunk to allow a uniform area of shielding and a guaranteed connection with the solder.

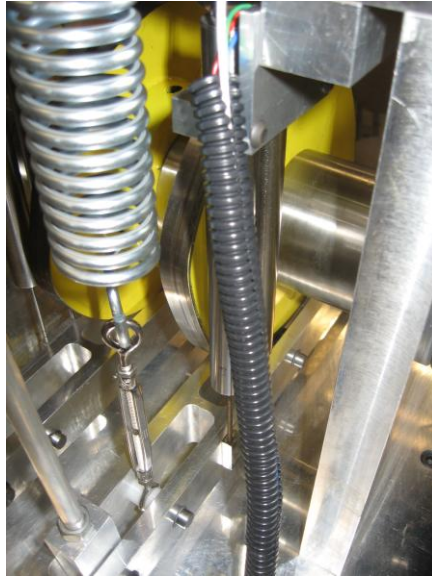


Figure 77

Figure 77 shows how constricting looms were used to contain the many wires coming out of the base plate and running to the sensors attached to the follower trains.

The new front panel plate located the remote motor controller conveniently at the mid-height of the machine. Figure 78 shows the DAQ input being tapped by a USB B to A cable.



Figure 78

All of the parts and systems that were designed were realized and assembled.



## 5. Conclusion

Due to the efforts of this project, the Cam Dynamics Test Machine at WPI can be used again as a demonstration of how cam-follower systems function and why they are used. The addition of the new DAQ has both improved the demonstration function of the CDTM and expanded the possibilities for experimentation and cam testing. The newly redesigned arms and trains allow faster cam speeds without detrimental deflection or contact between moving parts. All of the assemblies and tools associated with the machine can now be kept onboard. The electrical configuration is safer, and its specifications are documented. This Major Qualifying Project represents the culmination of the undergraduate educations of its authors, and the results will help others to learn.

## 6. Recommendations

The redesign of the Cam Dynamics Test Machine covered many areas, including the planning and realization of new follower trains, the improvement of the electronics and storage, and the restoration and enhancement of its ability to be used as a demonstration to students. As with any project, however, there is still a broad range of potential work to be done on or with the CDTM.

One area that could be expanded upon is data collection. The Virtual Instrument created in this project could be modified or improved. It does graphically display the data from each of the sensors simultaneously, but a more efficient way of writing the data to spreadsheet could be written. Also, more complex calculations using the data could be programmed into the VI, such as transforms. More sensors could be added and connected either internally or more temporarily through the extra inputs on the new front panel control plate as well to expand experimentation.

In terms of exploratory assignments, students could perform lab projects comparing the theoretical profiles, velocities, and accelerations of cams to the sensor outputs. They could also use theory to determine velocity or acceleration based on the position, or other such combinations, and determines which curve most closely matches the theory describing it.

New cams and associated follower trains could be designed, realized, and tested using CDTM also. The alternative trains, such as the translating follower train already with the machine, could be installed and tested. The natural frequencies of the various parts in the machine could be investigated as well, and the stiffness values could be compared to the theoretical values found through ProEngineer and DynaCam.

## 7. References

- 80/20 Inc. "T-Slot Framing." Updated 2005. Accessed November 19, 2008.  
<<http://www.8020.net/T-Slot-1.asp>>
- Albion, Inc. "16XS05201" Updated 2008. Accessed November 30, 2008.  
<<http://www.albioninc.com/index.php>>
- Drafts, Bill. "Acoustic Wave Technology Sensors." Sensors. 01 OCT 2001.  
Microsensor Systems. 16 Dec 2008  
< <http://www.sensorsmag.com/articles/1000/68/main.shtml>>
- Dytran Instruments. "Accelerometer 3145A" Updated 2008. Accessed January 13, 2009  
<<http://www.dytran.com/go.cfm/en-us/content/product/160/ACCELEROMETERIEPE-3145A/x?SID=>>>
- Munyon, Matthew A. "Design and Analysis of a Cam Dynamics Test Machine."  
Directed Research Project. Worcester Polytechnic Institute, December 2006.
- Northeastern University, "Digital Encoders." Encoders. 1999. 16 Dec 2008  
<[http://mechatronics.mech.northwestern.edu/design\\_ref/sensors/encoders.html](http://mechatronics.mech.northwestern.edu/design_ref/sensors/encoders.html)>
- Paradorn, Vasin "An Impact Model for the Industrial Cam-Follower System:  
Simulation and Experiment."  
Master's Thesis. Worcester Polytechnic Institute, October 2007.
- R+W Coupling Technology. "BLK-150" Updated 2008. Accessed December 3, 2008.  
<<http://www.rw-america.com>>
- Ruland Manufacturing, Inc. "SPX-16-12-F" Updated 2008. Accessed December 4, 2008  
<[http://www.ruland.com/ps\\_couplings\\_rigid\\_spx.asp](http://www.ruland.com/ps_couplings_rigid_spx.asp)>
- Sensor Technology Ltd.. "How Sensors Work - Transducers." 16 Dec 2008  
<<http://www.sensorland.com/HowPage008.html>>.
- Southco, Inc. "E6-10-501-20" Updated: 2008. Accessed: November 19, 2008  
<<http://www.southco.com/product/part.aspx?pn=E6-10-501-20>>

Staff, "Introduction to Accelerometers." OMEGA Technical Engineering Reference.  
OMEGA. 16 Dec 2008  
<<http://www.omega.com/prodinfo/accelerometers.html>>

WikiMedia Commons, "Animations of Machinery." Accessed January 10, 2009  
<[http://commons.wikimedia.org/wiki/Category:Animations\\_of\\_machinery](http://commons.wikimedia.org/wiki/Category:Animations_of_machinery)>

Zero-Max, Inc. "6P60C CD Hub" Updated: 2008. Accessed December 10, 2008.  
<[http://www.zero-max.com/products/cd/cd\\_df\\_clamp.asp](http://www.zero-max.com/products/cd/cd_df_clamp.asp)>

## Appendix A: Validation of the Finite Element Analysis

Prior to finalizing the design of the follower arm, the maximum deformation was estimated in order to gauge the ability of the arm to handle the loads it would encounter in use. The product specification that the maximum deformation experienced under loading should be 0.005 inches was used as a benchmark to compare with the estimated value. The value was also estimated using ANSYS with a simplified model using rectangular prismatic elements. Exporting the ProEngineer solid model of the part into ANSYS Workbench, a finite element analysis tool, allowed fairly accurate prediction of the deformation of the arm and whether or not this deformation was of an acceptable magnitude.

### A.1 Validation of the Software Value

Before the finite element analysis on the model was completed, calculations were performed outside of ProEngineer and ANSYS to determine a reasonable value for the deformation under the load. This guided the finite element analysis and acted as confirmation of the validity of the values generated by the software. Figure 79 illustrates the simplification of the arm for this by-hand calculation:

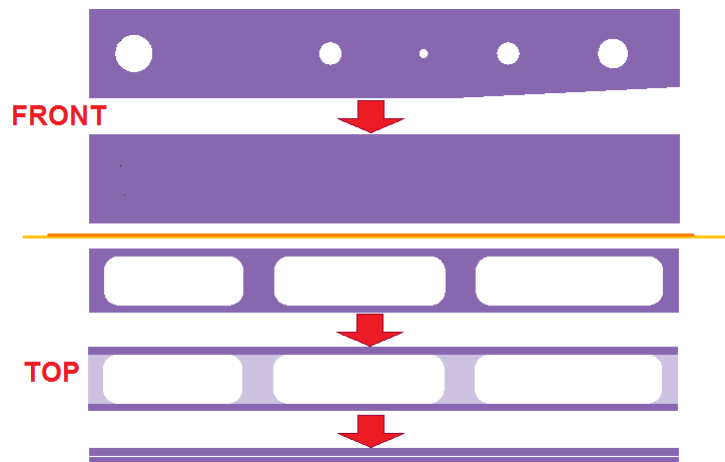


Figure 79

As is shown, the hole features were removed, the wedge-shaped cut was ignored, and the walls of the arm were considered as one rectangular cross-section without the four connecting sections between them.

To employ singularity functions in solving for the deformation, the loading and the relevant geometric properties were catalogued. Initially, some were kept as variables through the course of the calculation so that multiple iterations could be checked simply using the resulting equation. The simplified cross section of the arm, shown in Figure 80, was used as part of the geometric considerations of the by-hand calculation:

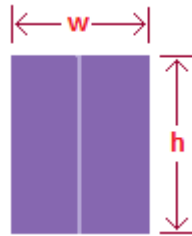


Figure 80

Where  $w$  is the width of the follower arm with the width of the well (.814 in) subtracted from it, and  $h$  is the height of the arm. Other geometric concerns were the lengths from the pivot block to the roller ( $a$ ), to the spring ( $b$ ), and to the end of the arm ( $l$ ), shown in Figure 81:

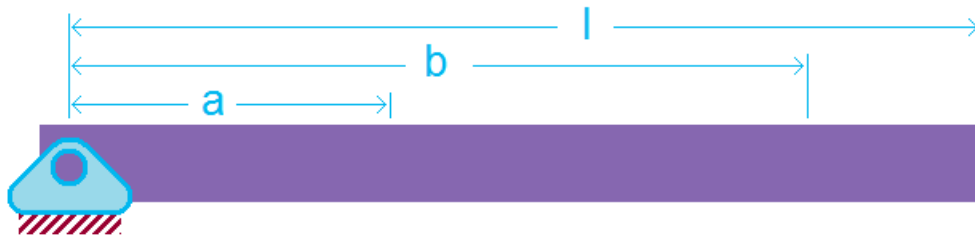


Figure 81

These were important lengths because they are the locations of the loading that is exerted on the follower arm. Due to the state of force and moment equilibrium on the beam and the assumption that the weight is negligible next to the forces applied, the reaction force and the spring force can both be calculated using the known reaction force of the cam on the follower,  $R_2$ , as determined using DynaCam. The following figure (Figure 82) and algebra show the value of the forces in relation to  $R_2$  and the geometric properties of the arm:

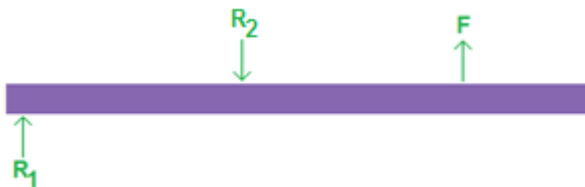


Figure 82

$$\Sigma M_{\text{pivot}} = 0 \therefore R_2 * a = F * b \therefore F = R_2 * (a/b)$$

$$\Sigma F_y = 0 \therefore R_1 + F = R_2 \therefore R_1 = R_2 - F \therefore R_1 = R_2 * [(b-a)/b]$$

The next step was to employ singularity functions. The loading of the beam, when expressed as a loading function, was integrated four times to find the deflection (see Machine Design or similar reference for the integration rules of singularity functions).

$$q(x) = R_1 * \langle x \rangle^{-1} - R_2 \langle x-a \rangle^{-1} + F \langle x-b \rangle^{-1} = R_2 * [([b-a]/b) * \langle x \rangle^{-1} - \langle x-a \rangle^{-1} + (a/b) * \langle x-b \rangle^{-1}]$$

$$\int q(x) = V(x) = R_2 * [([b-a]/b) * \langle x \rangle^0 - \langle x-a \rangle^0 + (a/b) * \langle x-b \rangle^0]$$

$$\int V(x) = M(x) = R_2 * [([b-a]/b) * \langle x \rangle^1 - \langle x-a \rangle^1 + (a/b) * \langle x-b \rangle^1]$$

Note: Constants of integration  $C_1$  and  $C_2$  were not shown because they are zero (no external loads).

The relationship between the angular displacement  $\Theta(x)$  and the moment function  $M(x)$  was as follows:

$$\Theta(x) = (1/EI) * \int M(x)$$

Where  $E$  was the Young's Modulus (in this case, 10,000,000 psi) and  $I$  was the area moment of inertia about the neutral axis of the beam:

$$I = [w(h)^3]/12$$

$$\text{Therefore, } \Theta(x) = (R_2/2EI) * [([b-a]/b) * \langle x \rangle^2 - \langle x-a \rangle^2 + (a/b) * \langle x-b \rangle^2 + C_3]$$

$$\int \Theta(x) = y(x) = (R_2/6EI) * [([b-a]/b) * \langle x \rangle^3 - \langle x-a \rangle^3 + (a/b) * \langle x-b \rangle^3 + C_3 * x + C_4]$$

The boundary conditions were another area of concern. Since the joint at the pivot was a pin joint, and the system was simplified from dynamic to static, it was necessary to specify at least two boundary conditions to ascertain the deflection result. The assumption was made that at the moment when the cam exerts the greatest force on the roller (and thus the follower arm), the spring prevents the roller from jumping off the surface of the cam. Therefore, regardless of the orientation of the follower arm with respect to the ground, the deflection can be said to be zero at the pivot and at the roller. In other words, the zero-line

(plane) about which the deflection will be measured is a line drawn from the pivot to the roller center, as shown in Figure 83:



Figure 83

$$y(0) = 0 = C_4$$

$$y(a) = 0 = \left[ \left( \frac{b-a}{b} \right) (a)^3 + C_3 * a \right]$$

$$C_3 = \left( \frac{a-b}{b} \right) (a)^2 = \left( \frac{a^3}{b} \right) + a^2$$

The end result of this calculation is the following general equation for the beam deflection at any point x:

$$y(x) = \left( \frac{R_2}{6EI} \right) * \left[ \left( \frac{b-a}{b} \right) * \langle x \rangle^3 - \langle x-a \rangle^3 + \left( \frac{a}{b} \right) * \langle x-b \rangle^3 + \left( \frac{a^3}{b} + a^2 \right) * x \right]$$

The shape of this curve is shown in

Figure 84. Note that the greatest deflection occurs at the end of the beam (length l).

### Deflection of the Beam with Respect to the Initial Neutral Plane

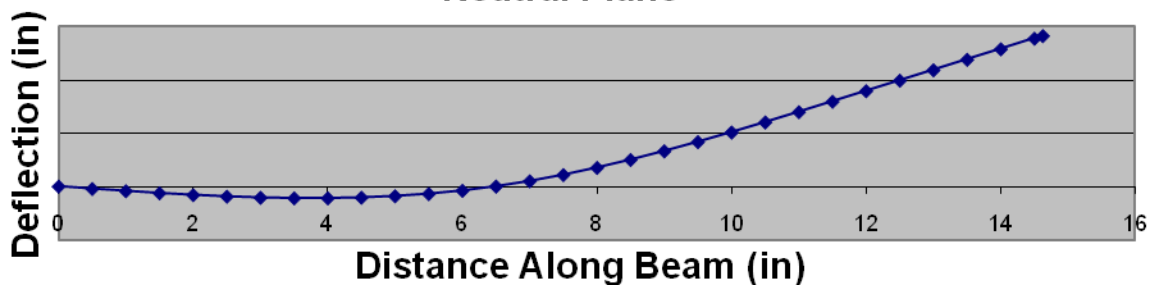


Figure 84



Table 5 shows the values used to calculate the deflection for one particular case:

**Table 5: The Values of the Variables Used to Complete Estimation**

Variable	Value
a	6.5 in
b	11.75 in
l	14.625
R <sub>2</sub>	92.192 lb
E	10000000 lbf/in <sup>2</sup>
w	.7 in
h	1.5 in
I	.197 in <sup>4</sup>

In this case, the calculated value of the greatest displacement came to:

$$y(14.625) = 0.00467 \text{ in}$$

The follower arm with 0.35” wall widths was brought into ANSYS Workbench and constrained in the same way. Figure sdsd shows the solved deflection value:

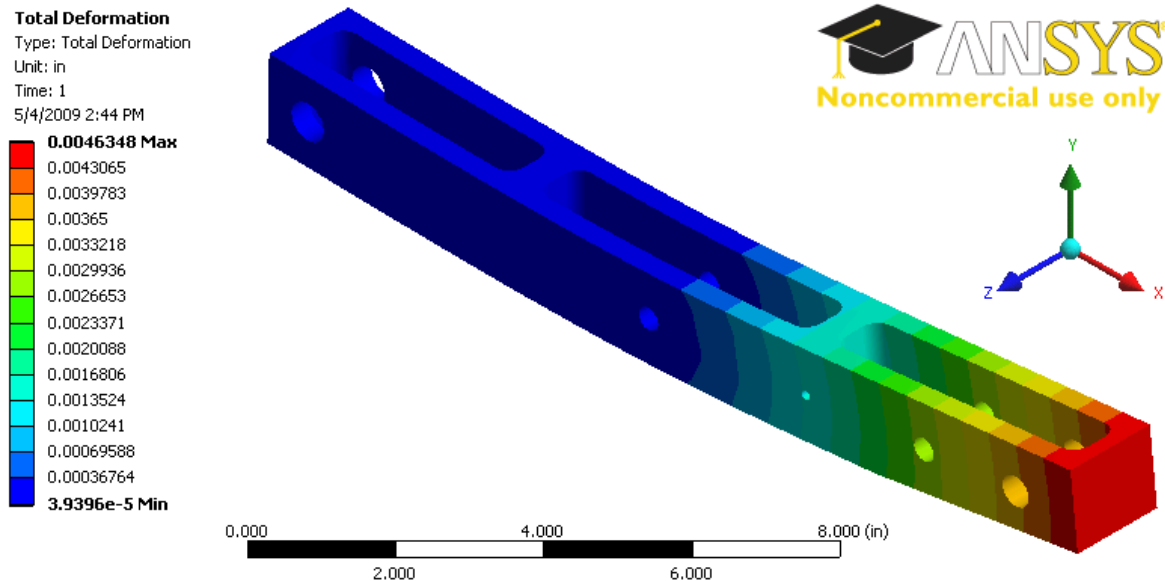


**Figure 85**

The value of the deflection at the tip was 0.00463 in. A comparable value to the simplified model was found for the same conditions in ANSYS Workbench when applied to the more complex model of the follower arm, and this validated the Workbench analysis.

## Appendix B: Axial Spacing in the New Design

The thickness of the three wells in the follower arm design was the same value, and that value was dictated by the thickness of the roller bearing being employed as the cam follower. That well thickness, in turn, dictated the thickness of the parts that were pinned to the follower arm in the wells (connecting to the spring and the connecting rod). The well thickness, with the added thickness of the two walls of the follower arm, dictated the thickness of the wells in the pivot block. Due to the consideration of tolerances and the need for some form of thrust bearing between the walls of pivoting elements and the wells that hold them, there was need for shims of varying (small) thickness and inner diameter to roughly center the pivoting elements in their wells. The details of the tolerances for each interaction and the associated washers are explained in this appendix. The calculations were completed with the assumption that the CNC machine tools of the shop that manufactured the non-standard parts were capable of maintaining dimensions to a tolerance of 0.001”.

### B.1 Roller Bearing within the Follower Arm Well

The roller thickness specifications are as follows:

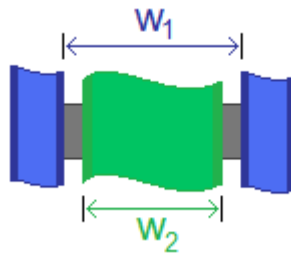


Figure 86

Where  $w_1$  is the well thickness and  $w_2$  is the thickness of the roller bearing.

$$w_2: 0.8115'' \leq w_2 \leq 0.813'' \quad (\text{According to McGill})$$

With a tolerance of 0.001”, the minimum well thickness must match the maximum thickness of the roller bearing.

$$\text{Therefore, } 0.813'' \leq w_1 \leq 0.815'', \quad \text{so the nominal } w_1 = 0.814''$$

In the best case, the minimum well width and the maximum bearing thickness would have made the bearing just fit without shims.

## B.2 Con-Rod - Follower Arm Connector within the Follower Arm Well

The thickness dimension of the connecting rod to follower arm pivot is as follows:

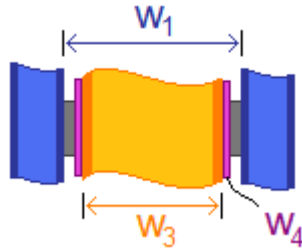


Figure 87

Where  $w_1$  is the well thickness,  $w_3$  is the thickness of the pivot, and  $w_4$  is the thickness of the low-friction washer.

In this case, the pivot has two low-friction washers between itself and the wall of the follower arm to limit the impact of its rotation on the wall.

The case with the maximum width of the low-friction washers (.035" each) and the minimum width of the follower arm well should yield the value of the maximum allowable width of the pivot:

$$.813'' - 2[.035''] = 0.743''$$

Therefore,  $0.741'' \leq w_3 \leq 0.743''$ , so the nominal  $w_3 = 0.742''$

The case with the maximum well thickness, the minimum pivot thickness, and the minimum low-friction washer thickness would yield the highest number of shims needed to locate the pivot centered on its shaft:

$$[0.815'' - 2(.027'') - 0.741''] / 0.001'' = 20$$

Luckily, in addition to the 0.001" thick shims, there were also 0.005" thick shims available – in this extreme case, two of them would be used on each side of each pivot block.

### B.3 Follower Arm within the Pivot Block Well

The thickness dimension of the connecting rod to follower arm pivot is as follows:

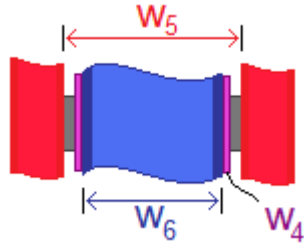


Figure 88

Where  $w_6$  is the follower arm thickness,  $w_5$  is the thickness of the pivot block well, and  $w_4$  is the thickness of the low-friction washer.

The follower arm thickness  $w_6 = w_1 + 2(\text{wall thickness})$ , where wall thickness = 0.5"

Therefore,  $1.813'' \leq w_6 \leq 1.815''$

In this case, the follower arm would have two low-friction washers between itself and the wall of the pivot block to limit the impact of its rotation on the wall.

The case with the maximum width of the low-friction washers (.035" each) and the maximum width of the follower arm should yield the value of the minimum allowable width of the pivot block well:

$$1.815'' + 2(.035'') = 1.885''$$

Therefore,  $1.885'' \leq w_3 \leq 1.887''$ , so the nominal  $w_3 = 1.886''$

The case with the maximum pivot block well thickness, the minimum follower arm thickness, and the minimum low-friction washer thickness would yield the highest number of shims needed to locate the pivot centered on its shaft:

$$[1.887'' - 2(0.027'') - 1.813''] / 0.001'' = 20$$

Luckily, in addition to the 0.001" thick shims, there are also 0.005" thick shims available – in this extreme case, two of them would be used on each side of each follower arm.

## Appendix C: Purchased Parts

Table 6: Bill of Purchased Parts

Part Name/Function	Part Number	Part Manufacturer
Motor	M3211-T50	Baldor
Motor Controller	ESV222N02YXC	AC Technology
Spring (Compensating)	LE 177L 02 M	Lee Spring
Spring (Primary)	LE 177N 01 S	Lee Spring
Turnbuckles	30315T611	McMaster Carr
Snap Rings 3/8" Shaft	SH-37ST PA	McMaster Carr
Snap Rings 1/2" Shaft	SH-50ST PA	McMaster Carr
Snap Ring Pliers	4621 A01	KNIPEX
Alloy 932 (SAE 660) Bronze Sleeve Bearing for 1/2" Shaft Diameter, 11/16" OD, 3" Length	6381K2	McMaster Carr
Teflon Washer - Inner Diameter = 0.527"	MSC #05404579	MSC Industrial Supply Company
Shim Washer - ID = 0.63", Thickness = 0.001"	MSC #05404967	MSC Industrial Supply Company
Shim Washer - ID = 0.63", Thickness = 0.005"	MSC #05405089	MSC Industrial Supply Company
Drop-In T-Nuts With Set Screw 5/16-18	3311	Air, Inc.
Wiring Duct 20.25"	2899	Air, Inc.
Standard T-Slot Covers - 72.5" Length	2111	Air, Inc.
6 Hole Inside Corner Bracket	4375	Air, Inc.
1530 Cap Ends Plain - Black	2030 - Plain	Air, Inc.
Extruded Bar	1530 Lite	Air, Inc.
Tool Steel Tight-Tolerance Rod 33/64 Diameter, 1' Length	8893K841	McMaster Carr
Socket Cap Screw 5/16"-18 Thread, 3/8" Length, Packs of 50	91255A576	McMaster Carr
Accelerometer	3145A	Dytran
Current Source	4114	Dytran
Threaded Hex Standoff 6mm Hex, 8mm Length, M3 Screw Size	98952A013	McMaster Carr
Button Head Socket Cap Screw M3 Size, 6 mm Length	92095A179	McMaster Carr
Flange Button Head Screw 8-32 Thread, 1/2" Length, Packs of 25	97654A104	McMaster Carr
XLR Cable Connectors HINGED COVER D-SIZE	568-SCDX	Mouser Electronics

USB Adapters USBA-USB B A BLACK HOUSING	568-NAUSB-B	Mouser Electronics
BNC Connectors Tee Adptr J/P/J-ECO	523-112461	Mouser Electronics
BNC Connectors BH ADAPT JACK/JACK	523-31-220N-RFX	Mouser Electronics
Button Head Socket Cap Screw 5/16"-18	91306A387	McMaster-Carr
Flat Head Socket Cap Screw 5/16"-18	91263A573	McMaster-Carr
3/4 Extension 304 SS Drawer Slide 20"L	12155A31	McMaster-Carr
NEMA L15-30, Power Lock Male Plug	9081T21	McMaster-Carr
Rain-Tight Outdoor Steel Enclosure (NEMA 3R)	7649K53	McMaster-Carr
NEMA L15-30, Power Lock Female Plug	9081T41	McMaster-Carr
Surge Suppressor with EMI Protection 8 outlet	7330K64	McMaster-Carr
Remote Wired Control for Motor Controller	ESV - ZXK1	AC Technology
Teflon Washer - Inner Diameter = 0.5"	MSC #05404348	MSC Industrial Supply Company
Shim Washer - ID = 0.38", Thickness = 0.001"	MSC #05404603	MSC Industrial Supply Company
Shim Washer - ID = 0.505", Thickness = 0.001"	MSC #05404785	MSC Industrial Supply Company
Shim Washer - ID = 0.505", Thickness = 0.005"	MSC #05404900	MSC Industrial Supply Company
Shoulder Screw - 1/4" Shoulder, Thread 10-24	MSC #78626108	MSC Industrial Supply Company
Torque Transducer	LXT 971	Cooper Instruments
Current Source	4114	Dytran
Accelerometer	3145A	Dytran
Optical Encoder	XH S35F - 100	BEI Technologies
Power Supply 1	T-40C	Meanwell
Power Supply 2	S-150-12	Meanwell
LVT	0112 0000	TransTech
LVDT	DC 750	Macro Sensors
Needle Bearing Follower Roller	CCYR 1-1/4	McGill
DAQ	USB-6229 BNC	National Instruments
Hinges	E6-10-501-20	SouthCo
Locked Caster	16XS05201R	Albion
Rotating Caster	16XS05201S	Albion
Coupling 1	BLK 150	R+W Coupling Technology
Coupling 2	SPX-16-12-F	Ruland Manufacturing
Coupling 3	6P60C CD Hub	Zero-Max